SCIENCE CHINA
Chemistry

• FEATURE ARTICLES •
• SPECIAL ISSUE • In Honor of the 100th Birthday of Prof. Khi-Rui Tsai

January 2015 Vol.58 No.1: 60–78
doi: 10.1007/s11426-014-5262-0

Molecular catalysis for the steam reforming of ethanol

Jianyi Lin*, Luwei Chen*, Catherine Kai Shin Choong, Ziyi Zhong & Lin Huang

Heterogeneous Catalysis, Institute of Chemical and Engineering Sciences Agency for Science, Technology and Research, Jurong Island 627833, Singapore

Received July 30, 2014; accepted October 20, 2014; published online December 8, 2014

In this paper, the application of molecular catalysis for steam reforming of ethanol (SRE) is reviewed. Eight metals (Ni, Co, Cu, Pt, Rh, Pd, Ir and Ru) have shown high catalytic activity for SRE. Among them Ni and Rh are very promising because of high d character in the metal bond and low metal-oxygen bonding (vs. metal-carbon). They can effectively promote C–C bond cleavage in the rate-determining process during SRE. However, Rh is weak in water-gas-shift so that CH_4 and CO become the main by-products at low reaction temperatures, while Ni catalysts suffer from rapid deactivation due to coking and sintering. Two low-temperature CO-free catalysts have been developed in our lab, namely Rh-Fe/Ca-Al_2O_3 and carbonyl-derived Rh-Co/CeO_2, in which the presence of iron oxide or Co can promote water-gas-shift reaction and significantly improve the SRE performance. On the other hand, adding 3 wt% CaO to Ni/Al_2O_3 can greatly improve the catalyst stability because the Ca modification not only increases Ni concentration on the Ni/Ca-Al_2O_3 surface and 3d valence electron density, but also facilitates the water adsorption and coke gasification via water-gas-shift. The availability of abundant surface OH groups helps the formation and conversion of adsorbed formate intermediate. Hence, ethanol reaction on Ca-Al_2O_3-supported Ni, Pt, Pd and Rh catalysts are found to follow the formate-intermediated pathway, a new reaction pathway alternative to the traditional acetate-intermediated pathway.

steam reforming of ethanol, molecular catalysis, hydrogen production, Rh catalysts, Ni catalysts, support effects, formate-intermediated pathway, Ca-Al_2O_3 support

1 Introduction

Ethanol as a feedstock for the production of H_2 is becoming more favorable with the increases in the energy demand, the price of fossil fuels, the CO_2 emission, and the feasibility of converting bio-mass into ethanol. Bio-ethanol is a renewable raw material and can be obtained from the fermentation of edible biomass such as sugarcane, corn and grains, or more recently from chemical conversion of nonfood biomass such as wood chips, agricultural crops, residues and wastes. Due to the latest technological breakthrough world ethanol production increases rapidly and its cost is continually decreased. Bio-ethanol-based H_2 production is considered to be a CO_2-neutral process because CO_2 produced by the ethanol production and reforming processes can be utilized for the biomass growth. Thus a closed carbon cycle could be established.

The steam reforming of ethanol (SRE) is a promising process to generate H_2, providing clean energy for the transportation and power plants. Stoichiometrically, each mole of ethanol can produce 6 mol of H_2 via the steam-reforming reaction:

$$C_2H_5OH+3H_2O \rightarrow 6H_2+2CO_2 \quad \Delta H=347.4 \text{ kJ/mol} \qquad (1)$$

When coupled with a H_2-O_2 fuel cell (FC), the efficiency of ethanol to energy via SRE is much higher than that via direct combustion of ethanol as a fuel. Energy balance calculations indicate that the same amount of ethanol can deliver about three times of energy by SRE/FC as compared to that via heat engine using blended gasoline-ethanol fuel [1].

In addition, as a liquid the storage, transportation and

*Corresponding authors (email: LIJY@ntu.edu.sg; chen_luwei@ices.a-star.edu.sg)

distribution of ethanol are easy. Unlike other liquid fuels such as methanol, diesel and gasoline, bio-ethanol is non-toxic, containing no sulfur that might poison the reforming and electrochemical catalysts. Therefore SRE has been extensively studied in recent years.

SRE is a good model system for fundamental molecular catalysis studies. Ethanol is the simplest molecule that contains single bonded C–C–O backbone. The reforming process of ethanol may involve the cleavage of O–H, C–H, C–C and (maybe) C–O bonds, as well as the formation or recombination of H–H, C–H and C–O bonds, which is more complex than the reforming of hydrocarbons. The molecular processes in SRE may proceed faster than hydrocarbon reforming in general, but still need the presence of an efficient catalyst that consists of both metal active phase and metal oxide support. Surface reactions or decompositions of ethanol and water on different metals or metal oxides significantly depend on their structural and electronic properties, resulting in different product distributions and variations of reaction mechanisms with different catalyst systems. These differences at first glance could be quite diverse. Nevertheless, a wealth of theoretical study, kinetic measurements and spectroscopic identifications of reaction intermediates have been reported during past three decades, providing evidence for the fundamental similarities in the reaction mechanisms and enabling the design of several good metal-oxide-supported metal catalysts with high ethanol conversion, H_2 selectivity and stability [2–9].

In this paper the application of molecular catalysis for SRE will be briefly reviewed in Sections 1–3 and the research efforts of our group in this topic will be summarized, mainly in Sections 4–6 [10–19].

2 SRE is kinetic controlled under normal conditions

To form CO_2 and H_2 from the reaction between ethanol and water there must be molecular processes including at least the cleavage of C–C, C–H and O–H bonds as well as the formation of H–H and C–O bonds. Methane and CO are thus the possible products, in addition to the final products, H_2 and CO_2. Thermodynamic analyses have revealed that SRE is entirely feasible [20–23]. But ethanol is unstable with respect to a mixture of H_2, CH_4, CO and CO_2, and may decompose according to the equations below:

$$2C_2H_5OH=3CH_4+CO_2 \quad \Delta H=-148 \text{ kJ/mol} \tag{2}$$

$$C_2H_5OH=CH_4+CO+H_2 \quad \Delta H=+49 \text{ kJ/mol} \tag{3}$$

Methane may also form from other pathways such as methanation reactions:

$$CO_2+4H_2=CH_4+2H_2O \quad \Delta H=-253 \text{ kJ/mol} \tag{4}$$

$$CO+3H_2=CH_4+H_2O \quad \Delta H=-251 \text{ kJ/mol} \tag{5}$$

In the presence of water, water-gas-shift (WGS) and methane steam reforming reactions may take place:

$$CO+H_2O=CO_2+H_2 \quad \Delta H=-41.2 \text{ kJ/mol} \tag{6}$$

$$CH_4+2H_2O=CO_2+4H_2 \quad \Delta H=253.2 \text{ kJ/mol} \tag{7}$$

The water-gas-shift (Eq. (6)) and methanation reactions (Eqs. (4) and (5), i.e. reversed methane reforming) are exothermic and hence favoured at low temperatures whereas methane steam reforming (Eq. (7)) is highly endothermic and thus feasible only at high temperatures. Thermodynamic analyses predict that H_2 is the predominant product in high temperature range (>780 K) while at lower temperatures undesired product CH_4 is predominant (Figure 1).

Actually some other reactions may also occur, producing the chemicals which are not shown in Figure 1. These include the dehydrogenation of ethanol to acetaldehyde (Eq. (8)) and the dehydration to ethylene (Eq. (9)):

$$C_2H_5OH=CH_3CHO+H_2 \quad \Delta H=+68 \text{ kJ/mol} \tag{8}$$

$$C_2H_5OH=C_2H_4+H_2O \quad \Delta H=+45 \text{ kJ/mol} \tag{9}$$

The products of these reactions are thermodynamically unstable with respect to the mixture of H_2, CO_2, CO and CH_4. They may undergo further reactions such as hydrogenation (Eq. (10)), decarbonylation (Eq. (11)), reforming (Eqs. (12) and (13)), polymerization (Eq. (14)) and dehydrogenations (Eq. (15)), eventually forming H_2, CO, CO_2, CH_4 and carbon deposits.

$$C_2H_4+H_2=C_2H_6 \tag{10}$$

$$CH_3CHO=CO+CH_4 \quad \Delta H=-19 \text{ kJ/mol} \tag{11}$$

$$CH_3CHO+H_2O=2CO+3H_2 \quad \Delta H=-55.8 \text{ kJ/mol} \tag{12}$$

$$C_2H_4+2H_2O=2CO+4H_2 \quad \Delta H=-36.9 \text{ kJ/mol} \tag{13}$$

$$C_2H_4 \rightarrow \text{polymer} \rightarrow \text{coke} \tag{14}$$

$$CH_4, C_2H_4, C_2H_6 \rightarrow C+H_2 \tag{15}$$

Boudouard reaction of CO can also take place, leading to

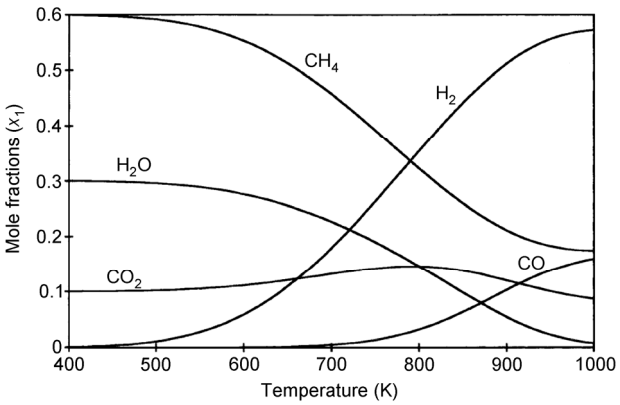

Figure 1 Species distributions as a function of temperature at p=1 atm, $n(C_2H_5OH)$=1 mol and $n(H_2O)$=3 mol obtained from Gibbs free energy minimization [20].

carbon formation:

$$CO+CO=CO_2+C \quad \Delta H=-171.5 \text{ kJ/mol} \qquad (16)$$

Hence C2 products such as acetaldehyde, ethylene and ethane will not be detected if the reactions proceed fast and the equilibrium could be achieved. However theoretical calculations and kinetic data show that the energy barriers for dehydrogenation and decomposition of ethanol are lower than those for the reforming of ethanol to H_2 and CO_2. Reactions (2) and (8) can occur well before Reaction (1) and proceed much faster than the reforming reactions, particularly in low temperature region. In a study of homogeneous non-catalytic ethanol reforming with a water:ethanol ratio of 3:1, ethanol was observed to form acetaldehyde and hydrogen as the predominant products at 200–550 °C [24]. The selectivity of acetaldehyde significantly dropped at 550 °C and approached zero at 650 °C. Methane and carbon monoxide productions were initially observed at 250–300 °C. The formations of ethane and ethylene were mainly observed at 550 °C and above. The dehydration of ethanol to ethylene may take place at lower temperature via monomolecular dehydration shown in Eq. (9). However, in gaseous phase the majority of ethylene presumably forms in a two-step intermolecular dehydration via the formation of diethyl ether ($C_2H_5OC_2H_5$) followed by a second dehydration of diethyl ether to ethylene, which requires higher temperatures. The selectivities of CO, CO_2, CH_4, C_2H_6, and C_2H_4 remained almost constant in high temperature range between 700 and 1000 °C. At such high temperatures, however, significant amount of carbonaceous deposits were formed from the polymerization and decomposition of ethane and ethylene, as well as the Boudouard reaction of CO and methane decompositions. These observations indicate that the product distribution of ethanol steam reforming is away from that of thermodynamic prediction and is kinetic-controlled under normal reaction conditions.

3 Combinatory catalysis and the best metal/oxide catalysts for SRE

For fast and selective (hence economically effective) conversion of ethanol to H_2, the SRE reaction requires a good catalyst, which should promote both reforming reaction and water-gas-shift reaction but inhibit the methanation and coke formation reactions, in particular when the reaction is performed at relatively low temperatures. Various types of catalysts have been used for SRE and well summarized in review papers [2–9]. Four groups of the catalysts are categorized [9], including metal oxides, metal-oxide-supported base metals (Ni, Co, Cu, Zn and Fe), noble metals (Pt, Rh, Pd, Ir, and Ru) and alloys (such as NiCu, RhCo, PtPd, etc.).

3.1 Metal oxide catalysts for SRE

Nine various metal oxides with a wide range of redox and acid-base properties have been tested by Llorca *et al*. [25] for SRE. Total (100%) ethanol conversion could be achieved on ZnO, Al_2O_3 and V_2O_5 (Figure 2).

However, only ZnO demonstrated good reforming performance, delivering 65% H_2, 21% CO_2 and 12% CH_3COCH_3 under the reaction condition of 723 K and 13:1 of steam:ethanol ratio. Al_2O_3, V_2O_5 and other oxides in this work show significant yields in the dehydration of ethanol and hence short catalytic life time due to the coke formation. On basic oxide MgO high selectivity to acetaldehyde is obtained. These findings are consistent with the acidic and basic characteristics of Al_2O_3 and MgO, respectively.

The excellent performance of ZnO in SRE could be a consequence of its dual (basic and redox) characteristics. The basic property of ZnO is in favour of the dehydrogenation of ethanol to ethoxy and then acetaldehyde through H-elimination over ZnO. The redox characteristics of ZnO could help to aid the conversion of acetaldehyde to acetate by nucleophilic attack of movable lattice oxygen. This in turn can be followed by hydride elimination to produce surface carboxylate which can further undergo decomposition to CO_2 and H_2 at higher temperatures [26,27]. Large amount of acetone is produced on ZnO via several successive reactions such as ethanol dehydrogenation and aldol condensation. The subsequent steam reforming of acetone can also generate H_2:

$$2C_2H_5OH=CH_3COCH_3+CO+3H_2 \qquad (17)$$

$$CH_3COCH_3+2H_2O=5H_2+3CO \qquad (18)$$

The CO selectivity on ZnO is almost zero, which could be attributed to the great activity of ZnO toward water-gas-shift reaction. Reducible oxides have been shown to greatly improve the activity of water-gas-shift catalysts as they could promote the dissociation of water, which is generally considered to be the key step in the reaction [28].

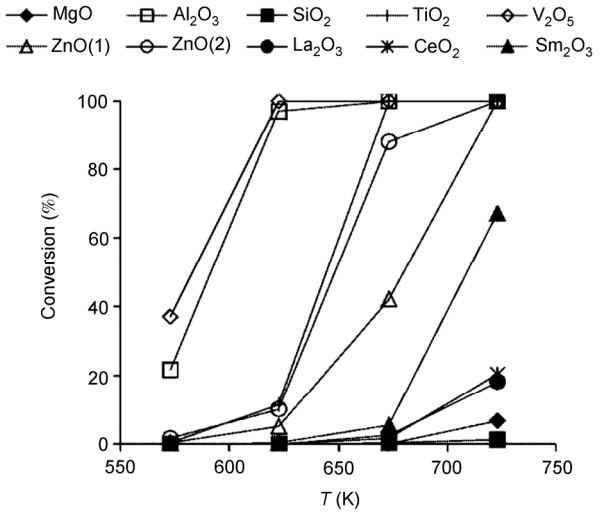

Figure 2 Ethanol conversion as a function of temperature for different oxides [25]. Reaction conditions: total pressure 1 atm, $C_2H_5OH:H_2:Ar$= 1:13:70 (molar ratio), GHSV=5000 h^{-1}.

Although ZnO alone is considered as the best metal-oxide catalyst for SRE, loading of 10 wt% Co on ZnO can significantly enhance the catalytic steam reforming of ethanol. The same group of researchers compared the SRE reactions on pure ZnO catalyst and ZnO-supported Co catalysts [25–27,29], showing that the presence of Co could promote the C–C bond scission and thus further improve the SRE activity and H_2 selectivity.

Very recently perovskite-type $La_{1-x}Ca_xFe_{1-x}Co_xO_3$ (x=0.3, 0.5) oxides were used for SRE and oxidative steam reforming of ethanol to produce hydrogen [30]. The catalyst is highly selective to hydrogen, as well as very stable for the reforming reaction. In the reaction process the cobalt species is possibly reduced to nanoparticles of metallic cobalt serving as the active center for SRE while the nano-Co particles can be oxidized back to the cobalt ions in the perovskite structure, leading to its high anti-sintering stability.

3.2 Active metals for SRE

3.2.1 The role of metal catalysts in SRE

The major role of a metal catalyst in SRE was well demonstrated in a recent study on Ni catalysts supported on CeO_2 at a constant ethanol/water ratio of 1:8 with stepwise heating to 300, 350, 400 and 450 °C, using combined *in-situ* DRIFT and XRD [31]. The simultaneous formation of CO_2 and H_2, as expected for SRE can be observed only at temperatures above 350 °C at which the NiO reduction to metallic Ni begins. When the fraction of metallic Ni in the catalyst increases from 0 to 24% during the stay at 350 °C, the H_2 production also increases. At 400 °C, the amount of Ni increases to 50% and stable at 58% while the activity accordingly increases and then remains stable for the rest of time at 400 °C, clearly indicating that metallic Ni is the active center for SRE. At 450 °C, over 85% of NiO is reduced, but sever carbon deposition causes clog of the reactor despite an initial boost of activity. The study also showed that Ni helps in the adsorption of the ethanol and in the cleavage of its C–C bond, while CeO_2 support facilitates the adsorption of water with the subsequent generation of OH groups which are essential for the reaction. The reaction pathway leads to CO_2 and H_2 predominantly via the formation of ethoxy, acetate, and carbonate surface species. On Ni/CeO_2, acetates start to break down at 350 °C, when NiO is reduced to Ni as seen in XRD. On pure CeO_2 without Ni, the formed acetates do not decompose and remain stable up to 400 °C. Without the CeO_2 support, acetates can still be decomposed by Ni, but with a significant production of CH_4 because of the insufficient supply of OH. Therefore, neither Ni nor CeO_2 can effectively transform the acetate to the desired gas products, CO_2 and H_2, by itself. The synergetic interaction of Ni and CeO_2 in the catalyst is important for the proper functioning of the catalyst [31]. Similarly, Cavallaro [32] showed the role of active metal in catalyzing the C–C bond breaking. With increasing the metal (Rh) loading on a Rh/Al_2O_3 catalyst for SRE, the amount of hydrogen formed increases, with a progressive increase in the C_1 products (CH_4, CO, and CO_2), while the C_2 products (ethylene, ethanol, and acetaldehyde) disappear gradually from the outlet gaseous stream.

3.2.2 Eight active metals (Pt, Rh, Pd, Ir, Ru, Ni, Co and Cu) for SRE

Recently combinatorial catalysis and high-throughput experimentation techniques have been used to design catalysts for low-temperature SRE. Duan *et al.* [33] evaluated 42 metals (from Groups I–V A, I–VII B and VIII in periodic table) having 4 different loadings (0.5 wt%, 1 wt%, 2.5 wt%, and 5 wt%) on five supports (Al_2O_3, SiO_2, TiO_2, CeO_2 and ZrO_2) for SRE at 573 K. A water/ethanol ratio of 6/1 was used. As evident from Figure 3 [33], most metals and support materials are inactive for ethanol conversion while only 7 metals from group VIII and group IB are active for SRE with an approximate activity ranking of Pt>Pd ≈ Rh>Cu ≈ Ni>Co ≈ Ir. The highest production rate of H_2 is observed for the 5 wt% Pt/CeO_2 catalyst.

Similar trend or ranking could be obtained from some papers which compared the performance of catalysts containing different metals dispersed over the same type of support. On γ-Al_2O_3 support, Auprêtre *et al.* [34] studied the SRE reaction at 700 °C over a series of metal catalysts (1 wt% Rh, 1 wt% Pt, 0.75 wt% Pd, 0.67 wt% Pt, 9.7 wt% Ni, 9.1 wt% Cu, 9.8 wt% Zn and 8.7 wt% Fe), showing Rh and Ni are the best catalysts, much better than other metals in a deceasing order of Rh ≈ Ni>Pd>Pt>Cu ≈ Zn>Ru in terms of H_2 yield (Table 1). Liguras *et al.* [35] investigated SRE at 650–800 °C over a series of γ-Al_2O_3-suported 1 wt% metal catalysts and came to similar trend: Rh≫Pt>Ru ≈ Pd.

At lower temperatures (300–450 °C), Basagiannis *et al.* [36] found that the catalytic performance varies in the order of γ-Al_2O_3-supported Pt>Pd>Rh>Ru, with Pt exhibiting high activity and selectivity toward hydrogen production, as well as long term stability at low temperatures. Chen *et al.* [17] prepared a series of bi-metallic Ni–Co catalysts supported on two types of metal-oxide supports, Ca-modified Al_2O_3 (Ca-Al_2O_3) and ZrO_2. Their results showed that Ni is a better SRE catalyst than Co on both the supports. In the entire temperature range between 500 and 800 °C, H_2 and CO_2 are the main products on 10% Ni/Ca-Al_2O_3 with almost zero of acetaldehyde. On the contrary, on 10% Co/Ca-Al_2O_3 the selectivity of acetaldehyde is as high as 50% at 500 °C, 25% at 600 °C and falls to zero only at 700 °C, indicating Ni is a much better catalyst than Co for the C–C and C–H bond breaking/activation. XRD study provided evidence that there exists no Ni-Co alloy formation on Ni-Co/Ca-Al_2O_3 due to strong metal support interaction. Hence the fact that the activity toward ethanol conversion and H_2 yield follows the sequence of 10% Ni>6.7% Ni-3.3% Co>3.3% Ni-6.7% Co>10% Co indicates that single-metallic Ni outperforms single-metallic Co catalyst while the bi-metallic

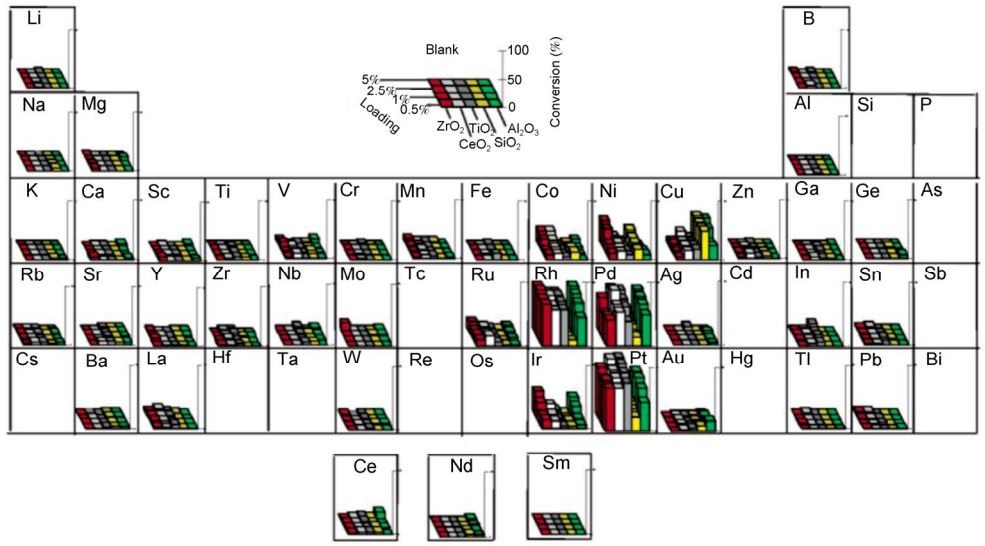

Figure 3 Ethanol conversion on supported single-component catalysts at 300 °C, 60000 h^{-1} of GHSV, and a 1:6 ethanol:H_2O molar ratio, diluted in 86% He [33].

Table 1 Ethanol steam reforming at 700 °C under stoichiometric reaction conditions ($n(H_2O)=3$, $n(C_2H_5OH)=1$) at atmospheric pressure on γ-Al_2O_3 supported Rh, Pt, Pd, Ru, Ni, Cu, Zn and Fe catalysts [34]

	Gas phase composition (%)						H_2 yield (g/(h g catalyst))	Selectivity towards CO_2 (%)
	H_2	CO_2	CO	CH_4	C_2H_4	C_2H_6		
Thermodynamic equilibrium	69.2	10	20	0.8	0	0	–	33
1% Rh/γ-Al_2O_3	72	21	7	0	0	0	2.3	75
1% Pt/γ-Al_2O_3	46	7	13	12	21	1	0.6	35
0.75% Pd/γ-Al_2O_3	55	2	18	15	9	1	1.1	10
0.67% Ru/γ-Al_2O_3	38	2	9	12	38	1	0.3	18
9.7% Ni/γ-Al_2O_3	70.5	18	11	0.5	0	0	3.1	62
9.1% Cu/γ-Al_2O_3	40	1	12	21	23	1	0.4	8
9.8% Zn/γ-Al_2O_3	42	0	16	21	20	1	0.4	0
8.7% Fe/γ-Al_2O_3	44	5	10	20	20	1	0.3	33

catalysts decrease its activity with increasing Co content.

Frusteri *et al*. [37] studied the performance of 3 wt% Rh/MgO, 3 wt% Pd/MgO, 21 wt% Ni/MgO, and 21 wt% Co/MgO catalysts for SRE. Rh and Ni catalysts showed the highest H_2 and CO_2 selectivities. Idriss [38] studied a series of CeO_2-supported metal and metal alloy catalysts, including Rh, Pt, Pd, Au, Pt-Rh, Rh-Au, Rh-Pd and Pt-Pd for ethanol reaction, indicating that hydrogen production from ethanol is directly related to two main steps. The first involves breaking the C–C bond, and Rh appears the most suitable compound for this reaction at reasonable operating temperatures. Ru catalysts do not always show high activity for SRE, particularly with low Ru loading. Koh *et al*. [10] prepared a series of alumina-supported 2.5 wt% Ru and Ru-Pt nanoparticles by the decarbonylation of organometallic cluster precursors. The organometallic-derived Ru catalysts were found to be highly active and selective to the formation of H_2 and CO_2, outperforming the 5 wt% Ru/Al_2O_3 catalysts prepared from inorganic salts using conventional impregnation method [10]. The highly dispersed nanoparticles derived from cluster precursors are much smaller (<2 nm) than the salt-derived nanoparticles which might account for the improved catalytic performance of the cluster-derived catalysts.

3.2.3 Theoretical calculation and model catalysts studies

Ferrin *et al*. [39] performed a DFT calculation of SRE on 10 metals (Cu, Pt, Pd, Ni, Ir, Rh, Co, Os, Ru, and Re) and experimental kinetic measurements on six carbon-supported metal catalysts to study the kinetic model of ethanol reforming. The results of DFT calculation predict that the rate constant for C–C bond cleavage in ethanol is much faster than for C–O bond cleavage on these metal surfaces at temperatures higher than 523 K so that the reforming is going through the C–C scission to form H_2 and CH_4. The trends in ethanol decomposition activity and selectivity on six of these metals: Cu, Pt, Pd, Ir, Rh, and Ru agrees well to experimental activity testing of the appropriate supported metal catalysts, showing that the C–C bond cleavage is significantly favored on these metals so that C_2H_6 via C–O

bond cleavage is ~2 orders of magnitude lower than that of CH_4 and CO production via C–C bond cleavage (Table 2) [39].

The rate-determining step in the reaction is the C–C bond breaking. Hence the metals which can better activate C–C bond are the better catalyst. Both experimental and DFT results show the activity order of Ru>Rh ≈ Pt>Pd>Ir>>Cu. On Cu, neither CH_4 nor CO nor ethane is observed in the effluent stream because the rates of C–O and C–C cleavage on Cu are very low, due to the low stability of all intermediates and related transition states [39]. The selectivity toward C–C cleavage (superior over C–O cleavage) on the five noble metals here results from the relatively weak bonding of O as compared with C on these surfaces. Since the transition state of C–O cleavage on metal surfaces contains a species bound through oxygen, the lower O binding on these surfaces means that the transition state of the adsorption is destabilized for C–O cleavage compared to C–C cleavage. This also provides an indicator that a metal with O binding closer to that of C binding would be better to selectively break the C–O bond [40].

Sinfelt *et al*. [41,42] studied the C–C bond activation on group VIII metals supported on silica. The order of catalytic activities is Ru>Ni>Rh>Ir>Co>Pd=Pt. The catalytic activity of the metals is well correlated to the d character in their metal bonds. Higher d percentage metals usually show higher C–C activity. As shown in Table 3 and Figure 4, basic metals Ni and Co have almost the same atomic radii 0.124/0.125 nm while noble metals have slightly large radii of 0.132–0.138 nm. They are hence only compared in two different groups.

From the above literature survey and molecular catalysis analysis it can be inferred that transition metals (M) of high d character and high M–C bonding stability, such as Rh and Ni can serve as a good catalyst for ethanol reforming due to their excellent capability in breaking the C–C bond of ethanol.

Surface science study has revealed that the bond-cleavage sequence in the surface reaction of ethanol on Ni(111) between 150 and 500 K is in the order of (i) H–O, (ii) H–αC (carbon in CH_2 group), (iii) C–C, and (iv) H–βC (C in CH_3) (Figure 5) [43]. Similar bond scission sequence was also observed on Pt(111), Pd(110) and Pd(111) surfaces etc. [44–46].

Table 2 Experimental results and model predictions for C–C and C–O bond-breaking turnover frequencies (TOF)

Metal	Experimental TOF (min^{-1})		Model TOF (min^{-1})	
	C–C cleavage	C–O cleavage	C–C cleavage	C–O cleavage
Cu	~0	~0	2.4×10^{-4}	3.3×10^{-6}
Pt	1.1	0.022	53	6.8×10^{-14}
Pd	0.52	0.002	23	4.7×10^{-14}
Ir	0.21	0.013	31	4.6×10^{-10}
Rh	0.95	0.002	164	8.9×10^{-6}
Ru	2.6	0.021	115	0.35

Table 3 Hydrogenolysis activitys of Group VIII metals in relation to other metallic properties [41]

Metal	Specific activity [a]	d character (%) [b]	Atomic radius [c] (Å)
First triad			
Fe	–	39.7	1.24
Co	4×10^{-5} [d]	39.5	1.25
Ni	7.9×10^{-4} [d]	40	1.24
Second triad			
Ru	3.2×10^{-2}	50	1.32
Rh	2.3×10^{-4}	50	1.34
Pd	7×10^{-10}	46	1.37
Third triad			
Os	–	49	1.34
Ir	1.1×10^{-4}	49	1.35
Pt	7×10^{-10} [d]	44	1.38

a) Moles ethane converted per hour per sq. meter at 205 °C; other conditions: p_{H_2} = 0.20 atm, p_E=0.030 atm; b) Pauling L. *Proc Roy Soc London*, 1949, A196: 343; c) Hume-Rothery W, Raynor GV. *The Structure of Metals and Alloys*. 4th Ed. London: The Institute of Metals, 1962, p95; d) Sinfelt JH, Taylor WF, Yates DJC. *J Phys Chem*, 1965, 69: 95.

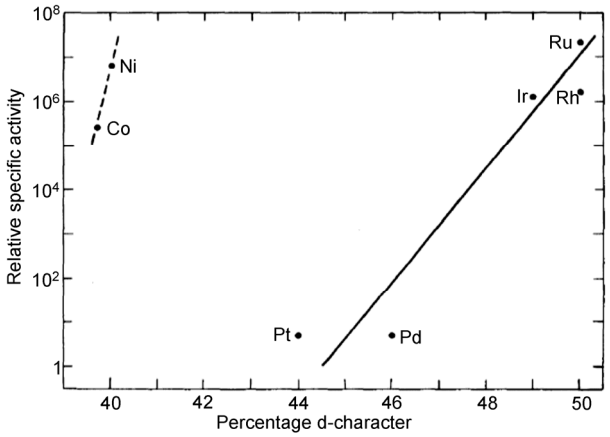

Figure 4 Specific activity (at 205 °C) of Group VIII metals for ethane hydrogenolysis as a function of d% character of the metal [41].

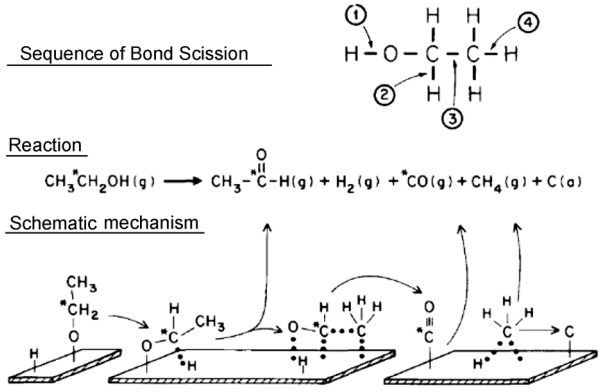

Figure 5 Summary of sequence of bond scission, product formed, and schematic mechanism for the decomposition and reaction of ethanol on Ni(111). The structures of the two intermediates at lower center are inferred [43].

For modeled Rh or supported Rh catalysts, another reaction pathway different from Ni and other noble metals (such as Pt and Pd) has been suggested [38,40]. The surface reaction of ethanol on Rh proceeds by the abstraction of a β-hydrogen, leading to the formation of a bidentate five-member oxametallacycle, Rh–CH_2–CH_2–O–Rh (here one Rh atom may be replaced by a metal ion of the oxide support such as Ce^{4+}), which is thermodynamically favourable and decompose to adsorbed CH_x and CO via C–C and C–H bond cleavage at higher temperatures. Rh is weak in water-gas-shift and steam reforming. Hence Rh usually shows significant formation of methane and CO, with a lower activity for the further conversion of methane and CO, as compared to Ni.

3.3 Support effects

Some studies have shown that metals alone do not assist H_2 production significantly and the performances of metal catalysts could be improved using suitable supporting materials [47,48]. Five different support effects have been summarized in literature [49], including dispersion effects, chemical effects, poisoning effects, electronic effects and bifunction effects. A good support for SRE should meet several requirements: (1) it should favor a good metal dispersion and stability; (2) it should be hydrophilic to promote water adsorption and activation; (3) it should assist the surface reaction to the desired reaction products on the metal particles via electronic or chemical effects; and (4) it should prevent coke formation via surface processes such as alcohol dehydration.

3.3.1 Bifunctionality

For the steam reforming reactions of ethanol the bifunctionality effect of the support is evident because metal oxide support can independently accommodate water, forming OH groups on the support surface. The support can also independently promote the ethanol decomposition, water-gas-shift and carbon formation reactions [9].

Ferencz *et al*. [49] studied SRE on Co catalysts supported on a series of various metal oxides. The activity and selectivity of Co-based catalysts were found to be more closely related to the chemical nature of the support than to the Co dispersion. On the acidic Co/Al_2O_3 catalyst, the highest ethanol conversion is detected at lower temperature. But ethylene is the main product and the hydrogen selectivity is almost zero. Furthermore acidic Al_2O_3 favors dehydration and thereby increases the tendency for coke formation due to the polymerization of ethylene. On Co/SiO_2 the dehydrogenation product acetaldehyde is one of the dominant products, but the conversion activity is rather poor. The dual-functional (basic and red-ox) Co/CeO_2 catalysts display high activity in SRE at 723 K, with hydrogen, acetone, CO_2, and CO being the main products. On basic CeO_2 dehydration is limited and its redox properties hindered coke formation. The easily accessible oxygen in CeO_2 can react with carbon species as soon as it forms, due to the high oxygen storage capacity and high oxygen mobility of CeO_2, which keeps the metal surface free of carbon, thus inhibiting deactivation. As a reducible metal oxide CeO_2 also promotes the water-gas-shift reaction. Hence Co/CeO_2 catalyst achieved high ethanol conversion and high selectivities (>90%) for H_2 and CO_2.

The bifunctional effect of supports is also demonstrated on Ni/CeO_2 [31,50]. Neither Ni nor CeO_2 can effectively transform stable surface intermediate acetate to CO_2 and H_2, by itself. On pure CeO_2, the acetates intermediate remains stable up to 400 °C, while without the CeO_2 support acetates can still be decomposed by Ni, but with a significant production of CH_4 because of the insufficient supply of OH. On the surface of Ni/CeO_2, ethoxy is 100% converted to acetate at 300 °C due to the presence of abundant OH groups on CeO_2 in the steam reforming atmosphere. Ni metal in close contact with CeO_2 is the active phase for SRE to H_2 and CO_2 at 350 °C. Ni is mainly responsible for cleaving C–C bonds of acetates or ethoxies, while Ce(III) sites produced by the Ni-CeO_2 interaction help to dissociate water, forming the surface OH groups that can react with methyl groups to form CO_2 rather than CH_4. Therefore CeO_2 support has two functions in addition to dispersing Ni particles: (1) facilitate the oxidation of ethoxies to acetates; (2) generate surface OH groups that promote the production of H_2 and CO_2 while inhibiting the formation of CH_4.

A good low temperature Rh/ZrO_2 catalyst for SRE was reported by Zhong *et al*. [11]. Pure ZrO_2 was found to be the best support at 300 °C with higher H_2 yield compared to the ZrO_2 oxide decorated with CeO_2, Al_2O_3, La_2O_3 or Li_2O, though at >450 °C, all the catalysts exhibited similar catalytic activity. Rh particle size and distribution, as well as the surface area of the catalyst, are not important factors in determining the catalytic performance while the preparation procedure of ZrO_2 could significantly enhance the catalytic activity, selectivity and stability. At 300 °C, high initial ethanol (EtOH) conversion (above 90%) and high H_2 yield (4.0 mol H_2/mol EtOH) were obtained on the catalyst prepared via a hydrothermal process (i.e. Rh/ZrO_2-HT) while low EtOH conversion (ca. 60%) and low H_2 yield (3.2 mol H_2/mol EtOH) were measured on Rh/ZrO_2-CP prepared by conventional co-precipitation. Both the catalysts at 300 °C gradually lose their activity, but Rh/ZrO_2-HT is more stable. NH_3-Temperature Program Desorption (TPD) was used to study the acidic sites on the two ZrO_2 supports, indicating the presence of two types of relatively strong acidic sites in ZrO_2-HT while only one type of weak acidic sites with lower concentration in ZrO_2-CP. After the aging test, the acidic sites are blocked by the deposit of the carbonaceous species on the spent Rh/ZrO_2 catalysts (Figure 6) [11].

In-situ diffusion reflectance infrared Fourier transfer spectroscopy (DRIFTS) studies for the ethanol adsorption

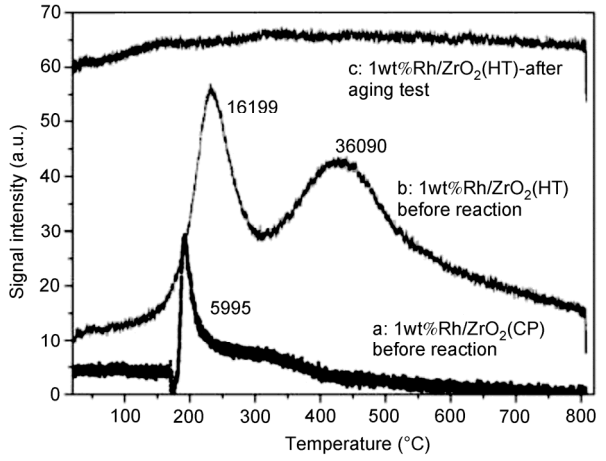

Figure 6 NH_3-desorption profiles of the two 1 wt% Rh/ZrO_2 ((a) for CP; (b) for HT, respectively) catalysts after reduced in 5%H_2 at 250 °C for 0.5 h (before reaction). (c) The 1 wt% Rh/ZrO_2-HT catalyst after the aging test [11].

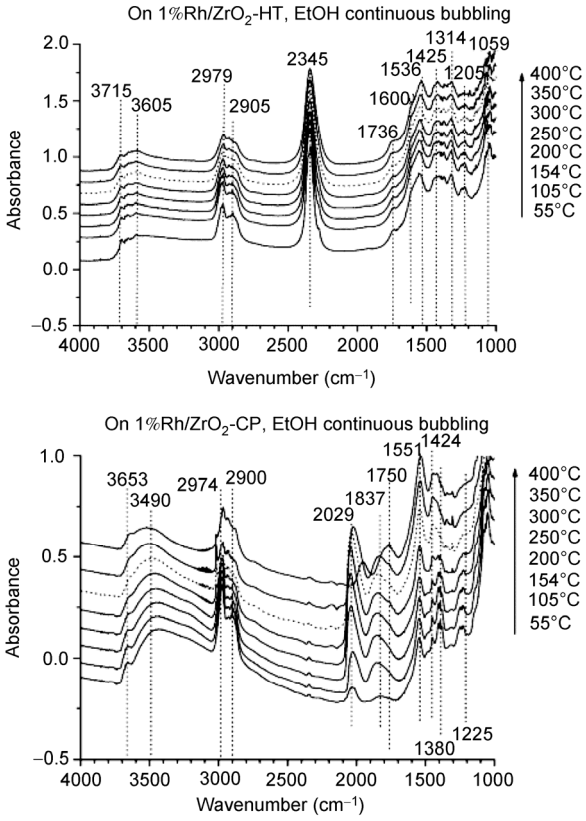

Figure 7 DRIFTS study of SRE on the two 1 wt% Rh/ZrO_2 catalysts [11]. (a) 1 wt% Rh/ZrO_2-HT; (b) 1 wt% Rh/ZrO_2-CP.

and reaction on the two catalysts at various temperatures show two remarkable differences in Figure 7 [11]. The peaks of O–H at 3605 and 3715 cm^{-1}, C–H (in CH_3) at 2905 and 2979 cm^{-1}, carboxylate COO at 1736 cm^{-1} and carbonate (mono- or/and bi-dentate) CO_3 at 1536, 1425, 1314, 1205 and 1059 cm^{-1} can be observed on Rh/ZrO_2-HT. The absence of the peaks between 2820 and 2840 cm^{-1} for H–αC (in CH_2) vibration indicates the rapid formation of acetyl species on the Rh/ZrO_2 (HT) catalyst even in low reaction temperature range via consecutive dehydrogenation reaction (C–H breakage reaction) on Rh particles. There is a strong CO_2 peak at 2345 cm^{-1} on Rh/ZrO_2-HT, which is absent on Rh/ZrO_2-CP. Meanwhile, there is only one type of OH group (bridging OH at 3653 cm^{-1}) on the Rh/ZrO_2-CP catalyst. The terminal OH at 3715 cm^{-1} is absent, while the CO peaks at 2029 cm^{-1} is rather strong on Rh/ZrO_2-CP. These may imply that more abundant OH groups on ZrO_2-HT facilitate the CO to CO_2 conversion via water-gas-shift on Rh/ZrO_2-HT. It is therefore concluded that the relatively strong Lewis acidic sites in the Rh/ZrO_2-HT catalyst are responsible for the strong absorption of EtOH molecules, and the subsequent C–H breakage step (leading to the formation of acetaldehyde) on Rh/ZrO_2-HT. On the Rh/ZrO_2-CP catalyst, the EtOH adsorption and water-gas-shift are weak due to the lack of abundant OH groups, and hence the C–C breakage is the dominating reaction which leads to the accumulation of surface CO and CH_x species.

3.3.2 Chemical and electronic effects

The chemical and electronic effects of supports have been carefully studied by Senanayake *et al*. [50] on Ni/CeO_2 using XPS, UPS and NEXAFS. The strong metal support interaction between Ni and CeO_2 leads to the partial reduction of the ceria substrate and the formation of Ni^{2+}, which existed as NiO and/or $Ce_{1-x}Ni_xO_{2-y}$. The electronic and chemical properties of Ni adatoms are thus affected, weakening their ability to break C–O bonds and substantially decreasing the CO methanation activity of Ni.

Oxygen spillover on the reducible oxides such as CeO_2, Ce-ZrO_2 or Ce-La_2O_3 composites was proposed in a study of SRE on Ni/Ce-ZrO_2 catalysts. This kind of oxides contains a high concentration of highly mobile oxygen vacancies at the metal-CeO_2 interface, which were considered as the active sites for the formation of oxygen or/and OH on its surface. The surface oxygen or OH species can spill over to react with reaction intermediates both from gaseous phase and on catalyst surfaces, effectively inhibiting the formation of hydrocarbons (CH_4, C_2H_4 and C_2H_6 etc.) and carbon deposits [24,51,52].

Duprez observed abundant OH groups on oxide surfaces, which migrate onto the metal particles through the metal/support interface. Once on the metal the OH groups react rapidly with hydrocarbon fragments, forming the final products [53]. Oxygen or OH mobility was found to be paralleled with the surface concentration of basic sites measured by CO_2 chemisorption in the order of CeO_2>MgO>ZrO_2>CeO_2-Al_2O_3>γ-Al_2O_3>SiO_2 [54]. Auprêtre *et al*. [34] tested Rh and Ni catalysts on a series of metal oxides and

found that on both the catalyst systems the activity in SRE decreases with deceasing the order of mobility of surface OH groups: $Ce_{0.63}Zr_{0.37}O_2$>CeO_2>CeO_2-γ-Al_2O_3>γ-Al_2O_3. Alumina-supported Rh is very active with 88% CO_2 selectivity, which can be attributed to the large adsorption capacity of alumina toward C_2H_5OH. But Al_2O_3 is selectively favors for the dehydration of ethanol to ethylene due to the acidic nature, which lowers the H_2 yield and deactivates the catalyst due to coking. On Rh/$Ce_{0.63}Zr_{0.37}O_2$, the formation of ethylene is limited while highest H_2 yield and relatively high CO_2 selectivity can be achieved. Hence Rh/Ce-ZrO_2 is one of the best SRE catalysts, which has attracted a lot of attention and studies.

3.4 Influences of reaction conditions

At high temperatures both thermodynamics and kinetics favor the complete ethanol conversion to H_2 and CO_2 production. But in low temperature region H_2 and CO_2 are thermodynamically unstable with respect to CH_4 and H_2O. Methane is a favorable product while the ethanol dehydrogenation and dehydration reactions catalyzed by the catalysts are much faster than the reforming reactions [39]. The coke formation due to the polymerization of ethylene (Eq. (14)) and the dehydrogenation reactions (Eq. (15)) are fast [8]. All the catalysts used for SRE produces CO. CO is a poison for many metal catalysts such as Rh and Pt. Additionally CO may lead to carbon deposition via Bourdouard reaction (Eq. (16)) leading to the deactivation of the catalysts. CO can be effectively converted to CO_2 and H_2 via water-gas-shift reaction. High water/ethanol ratio is thus in favor of the reforming and high H_2 yield. Nevertheless low temperature and low water/ethanol ratio are often desired to save the energy consumption.

Accordingly, stable selective hydrogen production via SRE would require an efficient catalyst that promotes reforming reactions (via C–C scission followed by water-gas shift) and inhibits methane-formation (via C–O scission followed by hydrogenation) and Bourdouard reactions, particularly when the reaction is performed in low temperature and low water/ethanol ratio range.

4 Development of CO-free Rh-based catalysts for low temperature SRE

As summarized in the aforementioned sections, Rh is highly active in C–C cleavage due to high d character in metal bond and hence is one of the best metal catalysts for SRE, better than other noble metals such as Pd and Ru [34,39]. However Rh is less active in converting CO and CH_4 via water-gas-shift and reforming reactions respectively. Hence further development of Rh catalysts must focus onto increasing the selectivity for H_2 production via water-gas-shift, while decreasing the selectivity for CH_4, CO and other undesired byproducts by using a suitable support or adding suitable promoters.

4.1 The Rh-Fe/Ca-Al_2O_3 catalyst for CO-free H_2 production at low temperatures

Chen *et al.* [13,14] reported a CO-free H_2 production through SRE at low temperatures between 623 and 673 K on iron promoted Rh catalyst supported on Ca-modified Al_2O_3 (Rh-Fe/Ca-Al_2O_3). As shown in Figure 8, without the Fe promoter, deactivation is observed for the Rh/Ca-Al_2O_3 catalyst after a 7.5 h reaction, accompanied by obvious increments in the CH_3CHO and CO selectivity; while with iron oxide, the high catalytic performance is well maintained for 288 h on Rh-Fe/Ca-Al_2O_3. In comparison with the Fe-free catalyst, both S_{CO_2} and Y_{H_2} increase significantly on the Rh-Fe/Ca-Al_2O_3 catalyst accompanying with the decrease in S_{CO}, while S_{CH_4} remains almost unchanged. Since iron oxide is a well-known water-gas-shift catalyst, it is reasonable to propose that the addition of iron oxides remarkably promotes the water-gas-shift, resulting in the improved hydrogen yield and reduced CO production at low temperatures. The conversion of CO was measured to be only 6% over the Rh/Ca-Al_2O_3 catalyst at 573 K, while it increased dramatically to 88% over the Rh-Fe/Ca-Al_2O_3 catalyst. The short life span of the Rh catalyst without Fe promoter is attributed to the poisoning effect of strong CO–Rh bonding and hence the blockage of Rh active sites for C–C bond activation and rupture.

In situ DRIFTS studies of CO adsorption support the above hypothesis. As shown in Figure 9, two strong bands at 2093 and 2020 cm^{-1} are observed for the Rh/Ca-Al_2O_3 catalyst. They are assigned to asymmetric and symmetric stretch of gem-dicarbonyls on Rh ions, respectively. The Rh–CO bond energy in gem-dicarbonyl is 145 kJ/mol, even

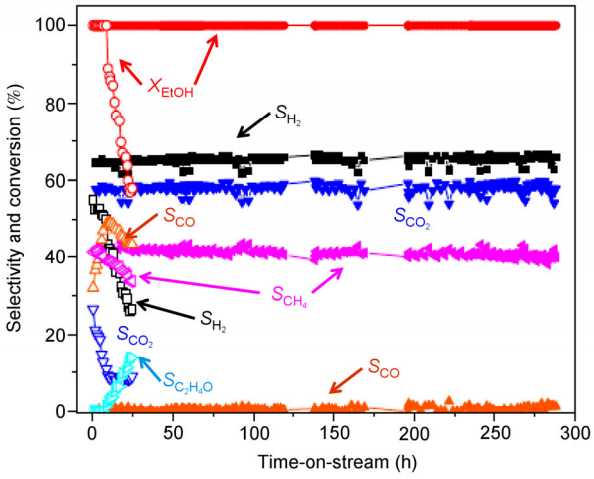

Figure 8 Comparison of ethanol and selectivity of products as function of time on stream over Rh-Fe/Ca-Al_2O_3 (solid) and Rh/Ca-Al_2O_3 (open) at 623 K and 1 atm [13].

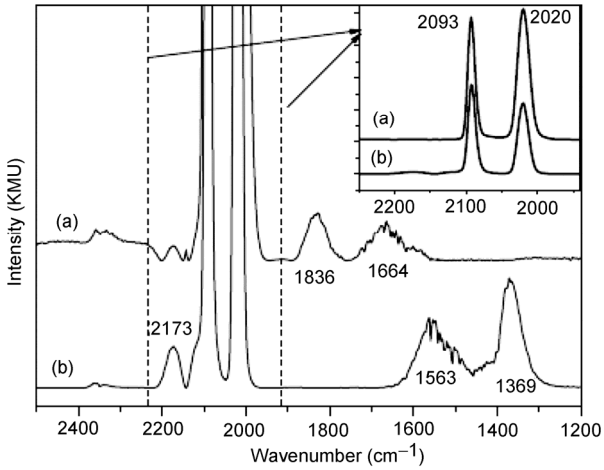

Figure 9 DRIFT spectra recorded under 1% CO/He at 298 K after H_2 treatment of Rh/Ca-Al_2O_3 (a) and Rh-Fe/Ca-Al_2O_3 (b) at 298 K [13].

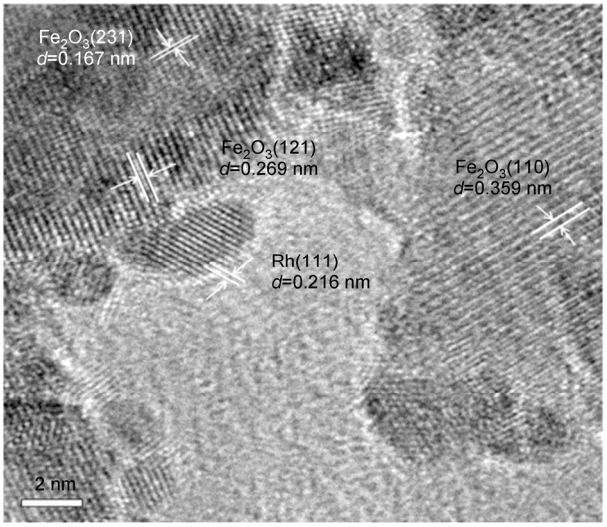

Figure 10 TEM image of Rh-Fe/Ca-Al_2O_3 catalyst (pre-reduced by H_2 at 473 K for 0.5 h) [13].

greater than the 121 kJ/mol of Rh–Rh bonds in metallic Rh. The high concentration of gem-dicarbonyl CO that may remain on the Rh surface at temperatures <503 K will poison the Rh active sites for ethanol adsorption and further acetaldehyde decomposition.

At higher temperatures, CO may undergo the Boudouard reaction, thus depositing carbon and poisoning the catalyst. For the Rh-Fe/Ca-Al_2O_3 catalyst, the concentration of gem-dicarbonyl CO is mitigated (inset of Figure 9) so that the CO poisoning effect can be reduced. Two smaller bands at 1836 and 1664 cm^{-1} in Figure 9(a) can be attributed to bridged Rh_2-CO and tilted CO. The other smaller bands at 2141 and 2172 cm^{-1} can be assigned to $Rh^{2+}(CO)_2$. It is noted that in Figure 9(b) two new bands at 1563 and 1369 cm^{-1} are evidently observed, which can be attributed to the formate species HCOO on iron oxide surface. These peak changes suggest that adsorbed CO species on Rh sites can be converted to HCOO species in the presence of iron oxide, which is an excellent catalyst for the water-gas-shift and is now located adjacent to Rh, as shown by the TEM image in Figure 10.

Characterization by X-ray absorption near edge spectroscopy (XANES) indicates the presence of Fe_xO_y species (~12% Fe, 43% Fe_3O_4 and 45% Fe_2O_3) upon reduction (Figure 11), resulting in the formation of coordinatively unsaturated ferrous (CUF) active sites along the Rh-Fe_xO_y interface. These CUF sites promote water-gas shift reaction during low temperature SRE [14]. The results clearly indicate that in the presence of iron oxide, adsorbed CO species on Rh sites can be converted to gaseous CO_2 or adsorbed HCOO species which can be further converted to H_2 and CO_2 so that the H_2 and CO_2 yields are increased significantly.

4.2 Bi-metallic Rh-Co catalyst supported on CeO_2 for CO-free H_2 production at low temperatures

In 2013 Huang *et al.* [12] reported that bimetallic Rh-Co catalysts supported on CeO_2 can improve the water-gas-shift capability of Rh-based catalysts and achieved CO-free,

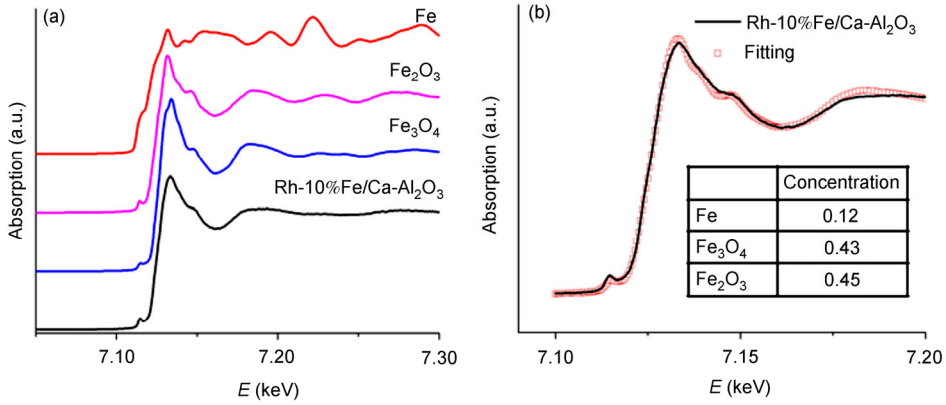

Figure 11 (a) Fe K-edge XANES spectra of reference compounds and Rh-10% Fe/Ca-Al_2O_3 catalyst; (b) Fe K-edge XANES spectrum of the reduced Rh-10% Fe/Ca-Al_2O_3 catalyst along with a weighted linear combination of XANES spectra of reference compounds. The inset in (b) shows the composition of iron species on the reduced catalyst [14].

high yield H_2 production at low temperature (300 °C). Five CeO_2-supported bimetallic catalysts were prepared from Rh and Co carbonyl precursors with the Rh/Co molar ratios decreasing from 3, 2, 1.5, 1 to 0.5. The overall activity of the five Rh-Co catalysts for the SRE at 300–400 °C is generally similar to that of single-metal Rh/CeO_2 in terms of C_2H_5OH conversion and H_2 yield. However, the selectivity to CH_3CHO rises with increasing Co/Rh atomic ratio, while the selectivity to CO declines to a different extent compared to that on Rh/CeO_2, in favor of the increase of selectivity to CO_2. These imply that the addition of Co as the second metallic component promotes the dehydrogenation, water-gas-shift and reforming reactions. It is generally accepted that on Rh catalysts ethanol is first converted to bi-dentate adsorbed oxametallacycle Rh–CH_2–CH_2–O–Rh via H-elimination, which is followed by C–C bond breaking to form CH_4 and CO. Rh is strong in C–C bond cleavage but weak in reforming and water-gas-shift, resulting in high selectivity of unwanted CH_4 and CO. The presence of the second metal catalyst Co enhances the capability of dehydrogenation, reforming and water-gas-shift since Co, like Ni, is more active than Rh in both the reactions [8]. Indeed, the increase of selectivity to CH_3CHO with increasing Co content is an indication that the addition of Co shifts the process gradually from EDO [ethanol (via) dehydrogenation (to) oxametallacycl] to EDA [ethanol (via) dehydrogenation (to) acetaldehyde]. At the same time, the selectivity to CH_4 decreases significantly with increasing Co/Rh atomic ratio at 250–350 °C, indicating the occurrence of acetaldehyde reforming in competition with the decomposition of acetaldehyde (to CH_4+CO) in the presence of Co. Notably, there is an optimized Co/Rh ratio of 1.5:1. In the temperature range of 300–400 °C a negligible selectivity to CO and decreased selectivity to CH_4 are observed on the Rh-Co catalyst with 1.5 of the Co/Rh ratio with the concurrent H_2 yield of 4.27–4.76 mol H_2 per mol C_2H_5OH. The catalysts of other ratios need higher temperatures to totally remove CO. An array of the SRE bi-layered catalysts were designed and compare, showing that the above carbonyl-derived bimetallic Rh-Co/ZrO_2 catalysts are better than those composed of physically mixed two single-metal (Rh/CeO_2 and Co/CeO_2) catalysts or the two single-metal catalysts arranged in a bi-layer configuration, indicating the synergistic effect occurs between Rh and Co. XPS study revealed that strong interaction between Rh and Co in the carbonyl-derived Rh-Co/CeO_2 catalysts results in the enrichment of both Rh and Co metals on the catalyst surface as compared to those Rh-Co/CeO_2 catalysts prepared from Rh and Co nitrates via conventional co-precipitaion procedure. After the SRE reaction Rh is basically maintained at metallic state while Co is fully oxidized to Co^{2+}, which is attributed to the water oxidation and may imply that Co is the active center for water-gas-shift, leading to the production of CO-free, low-CH_4 and high-yield H_2.

5 Development of coking-resistant Ni/Ca-Al_2O_3 catalysts for SRE

Aside from noble metals, Ni is so far the best non-noble metal catalyst for SRE to hydrogen production. Ni has high activity for C–C bond and O–H bond breaking and also has high activity for hydrogenation and water-gas-shift, facilitating H atoms to form molecular H_2 and converting CO to CO_2. Hence Ni is very promising with the catalytic activity compatible to or better than Co, Rh, Pt, Pd and Ru while it is more economical than Co and noble metal catalysts. However Ni suffers from coke formation as well as metal sintering, leading to considerable performance degradation during long-term operation. Hence research on Ni catalyst development will be fruitful, focusing to the improvement of catalyst stability.

To date, the use of Ni-based catalysts supported on Al_2O_3 seems to be a popular and excellent material for SRE since both Ni and Al_2O_3 are cheaper alternatives to their expensive counterparts such as the noble metals as well as CeO_2, ZnO and ZrO_2 supports. Rostrup-Nielsen [55] have pointed out that Ni on Al_2O_3 has substantially higher activity than Ni supported on either SiO_2 or carbon because water is mainly activated on the hydrophilic surface of the support. Therefore, supports that can readily and reversibly interact with water, such as alumina, are superior to those supports such as SiO_2 which have only tightly bound hydroxyl groups or carbons which probably have only a few sites that might accommodate the type of dissociative water [55]. Alumina can accommodate large amount of water and is an excellent support for metal catalysts including Ni. However the strong acidic nature makes Al_2O_3 alone not suitable for SRE because it promotes dehydration reaction of ethanol to ethylene which undergoes polymerization forming coke to deactivate the metal catalysts rapidly.

5.1 SRE on bare Al_2O_3 and Ca-modified Al_2O_3 supports

Choong *et al*. [15,16] studied SRE on γ-Al_2O_3 without Ni. The ethanol conversion is relatively high (59.3%). However, little H_2 (2%) is yielded and most of ethanol are converted to C_2H_4 (88.7%) and CH_3CHO (11.3%). To improve the catalyst stability by depressing the acidity of alumina CaO was introduced to alumina and minimized the dehydration of ethanol on the alumina support. Calcium is a well known alkaline earth metal with basic property and has been used as a catalyst promoter by various research groups in different kinds of reactions, such as methane dry reforming, Fischer-Tropsch synthesis, propane dehydrogenation and dehydrosulfurization of petroleum feedstock, led to positive catalytic effect in terms of higher activity and coking resistance. As summarised in Table 4 [15], the addition of CaO greatly reduces the ethanol conversion in SRE on the

Table 4 Catalytic performance on various catalyst at 673 K [15]

Catalyst	X_{EtOH} (%)	S_{H_2}	Y_{H_2} (mol)	Product distribution (%)				
				S_{CO_2}	$S_{C_2H_4}$	$S_{C_2H_4O}$	S_{CH_4}	S_{CO}
Al_2O_3	59.3	2.13	0.08	0	88.7	11.3	0	0
3Ca-Al_2O_3	7.60	22.2	0.10	0	7.71	92.3	0	0
7Ca-Al_2O_3	4.48	30.1	0.08	3.45	8.03	88.5	0	0
1Ni/Al_2O_3	83.9	45.5	2.29	2.74	13.5	37.9	18.5	27.3
1Ni/3Ca-Al_2O_3	100	73.2	4.39	59.4	0	0.91	33.5	6.21
1Ni/7Ca-Al_2O_3	97.9	67.3	3.96	44.9	0	9.00	32.8	13.3

Ca-Al_2O_3 supports, which drops drastically from 59.3% on bare alumina to 7.6% and 4.5% on 3Ca-Al_2O_3 (3 wt% Ca addition) and 7Ca-Al_2O_3 (7 wt% Ca addition), respectively. The formation of C_2H_4 is also suppressed greatly from 88.7% on bare alumina to 8% on Ca-Al_2O_3 supports. The H_2-yield is <0.1 mole per mole of ethanol on all the three alumina supports. These results conclude that both Al_2O_3 and Ca-Al_2O_3 supports are not active for ethanol steam reforming and the Ca addition greatly suppresses the dehydration of ethanol to C_2H_4 on Al_2O_3 support.

DRIFTS studies indicate that there are two types of OH groups on γ-Al_2O_3 (Figure 12): Type IIb (bridging) OH at 3752 cm^{-1} and acidic Type III OH group (involving three octahedrally coordinated Al^{3+} ions) at 3678 cm^{-1}. The broad absorption bands between 3540 and 3250 cm^{-1} on Ca-Al_2O_3 are attributed to H-bonded OH groups and suggest that CaO promotes the adsoprion/absoprion of water and enhance the affinity of the oxide support for H_2O molecules.

NH_3-TPD was used to examine the acidic property of the Ca-modified supports. On bare Al_2O_3, the NH_3-TPD profile (Figure 13) shows a strong peak around 423 K and a broad desorption shoulder tailing to 773 K, which can be assigned to the desorption of adsorbed NH_3 molecules from Lewis-acid sites of various strength, including coordination-unsaturated Al^{3+} ions which are the strongest acid sites. On Ca-Al_2O_3 supports, symmetrical desorption peaks without high temperature tail in Figure 13(b, c) suggests the elimination of high-acidity sites of Al_2O_3. The low temperature peak around 423 K decays significantly from 439.4 mol/g for bare Al_2O_3 to 164.8 mol/g for 3Ca-Al_2O_3 and finally decreases to 63.9 mol/g for 7Ca-Al_2O_3. This indicates that CaO is effective in reducing the density and the strength of acidic sites of the Al_2O_3 support. The addition of CaO not only depletes the acidic OH groups but also eliminates coordinatively unsaturated surface Al^{3+} ions.

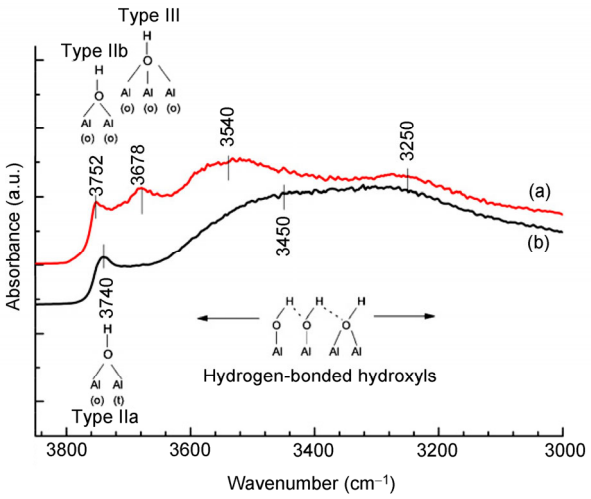

Figure 12 The DRIFTS spectra in the region between 3000 and 3800 cm^{-1} of the catalyst supports. (a) Al_2O_3; (b) Ca-Al_2O_3. Al(o) stands for octahedrally coordinated Al^{3+} ions while Al(t) for tetrahedrally Al^{3+} ions [15].

5.2 SRE on low loading (1 wt%) Ni/Al_2O_3 and Ni/Ca-Al_2O_3

Low loading (1 wt%) of Ni was supported on three alumina supports with various Ca-weight percent modification, i.e. *x*Ca-Al_2O_3 (*x*=0, 3 and 7) to demonstrate the role of Ni and the support effects in SRE. At such low nickel loading, the system is less likely to fall within the equilibrium limited region, enabling better comparison of the CaO addition with different amounts. At high temperatures of 723–873 K, all three Ni catalysts, i.e. 1 wt% Ni/Al_2O_3, 1 wt% Ni/3Ca-Al_2O_3 and 1 wt% 7Ca-Al_2O_3, attain 100% ethanol conversion. However, at a relatively low temperature of 673 K, the ethanol conversion (X_{EtOH}) and H_2-yield (Y_{H_2}) on the three supports are found to be different, increasing from X_{EtOH}= 59.3%/Y_{H_2} =0.08 for bare Al_2O_3 to 84%/2.29 for Ni/Al_2O_3,

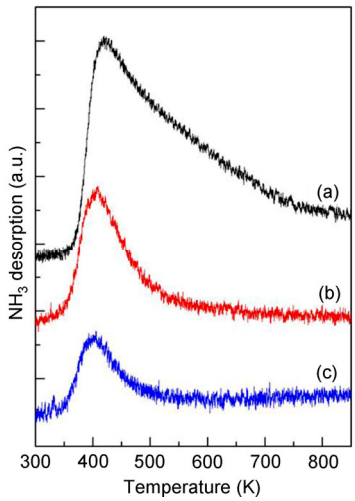

Figure 13 NH_3-TPD of the catalyst supports [15]. (a) Al_2O_3; (b) 3Ca-Al_2O_3; (c) 7Ca-Al_2O_3.

100%/4.39 for Ni/3Ca-Al_2O_3 and 98%/3.96 for Ni/7Ca-Al_2O_3. Ni promotes the conversion of ethanol while the addition of CaO further enhances the catalytic activity of the catalysts. The product distributions listed in Table 4 are greatly different too, depending on the CaO content. High ethylene and acetaldehyde selectivities are observed on Ni/Al_2O_3. On Ni/Ca-Al_2O_3, hydrogen selectivity increases significantly from 45% on Ni/Al_2O_3 to 67%–73% on Ni/Ca-Al_2O_3, while the ethylene formation depresses. The acetaldehyde selectivity is rather low too. It appears that in the presence of Ni ethanol and the related reaction intermediate CH_3CHO undergo decarbonylation (via C–C bond breaking), giving CH_4 and CO. CO can be further converted to H_2 and CO_2 (via water-gas-shift) or to carbon deposition (via Bourduard reaction). The Ca modification promotes these reactions so that the major products on Ni/Ca-Al_2O_3 at 673 K are H_2, CO_2 and CH_4. In terms of H_2 yield, Ni/3Ca-Al_2O_3 is the best catalyst among the three Ni catalysts.

In situ DRIFT spectra of ethanol adsorption on Al_2O_3, Ca-Al_2O_3 and Ni/Ca-Al_2O_3 at various temperatures in Figure 14 reveal a reaction pathway in which Ni promotes the C–C bond cleavage via formation of formate. On bare Al_2O_3 the adsorption of ethanol at room temperature generates the IR bands at 2966, 2926, 2875 and 1386 cm^{-1}, which are ascribed to $\nu_a(CH_3)$, $\nu_a(CH_2)$, $\nu_s(CH_3)$ and $\delta(CH_3)$, respectively, implying the existence of surface ethoxide species. On the same spectrum the OH bands at 3752 and 3689 cm^{-1} decrease their intensity upon the ethanol adsorption, indicating that the ethoxide species are attached to the support at the expenses of type II and type III OH groups. Note that the disappearance of $\nu_a(CH_2)$ at 2923 cm^{-1} is faster than $\nu_a(CH_3)/\nu_s(CH_3)$ at 2968/2872 cm^{-1}, which may imply the αC–H bond is preferably ruptured, forming acetaldehyde and acetyl intermediates. The acetaldehyde C–H band appears at 2735 cm^{-1}. The ethoxide and acetaldehyde bands are stable up to 573 K. They completely disappear from Al_2O_3 at 673 K while the OH bands at 3689 and 3752 cm^{-1} re-appear. Ethylene is the main product for SRE on pure Al_2O_3 in this temperature range (Table 4). The desorption of ethylene from adsorbed ethanol on bare Al_2O_3 may proceed via the C–O and βC–H bond scissions. Nevertheless at 673 K, new IR bands at 1575 and 1456 cm^{-1} which are attributed to acetate species may suggest that at 673 K the ethoxide or acetaldehyde species are converted to surface acetate. Surface acetate species can derive from the reaction between surface OH and adsorbed acetaldehyde. On bare Ca-Al_2O_3 support without Ni, ethoxide and acetaldehyde adsorbed species are similarly observable. They are more stable than that on pure Al_2O_3 and remain observable at 673 K. In addition, no acetate species are detectable. These indicate that Ca modification can stabilize ethoxide and acetaldehyde species due to the reduction of the surface acidity. At 673 K acetaldehyde is the main product ($S_{acetaldehyde}$= 88.5%–92.3%) of SRE on Ca-Al_2O_3 (Table 4). On Ni/Ca-Al_2O_3 the ethoxide and acetaldehyde species are observable only between 300 and 523 K. Their IR intensity falls to zero at 573 K, which is significantly lower than those (673 K and above) on bare Al_2O_3 or Ca-Al_2O_3 supports without Ni. At 523–673 K new IR bands at 1575 and 1349 $cm^{-1}$are strong on Ni/Ca-Al_2O_3, which can be assigned to ν_a(O–C–O) and ν_s(O–C–O) of adsorbed formate spices, respectively, clearly indicating the conversion of C_2 intermediates (CH_3CHO or CH_3CO) to C1 intermediate (HCOO) via C–C bondbreaking promoted by Ni. In the same temperature region, the H-bonded OH band in 3000–3600 cm^{-1} decays in intensity, meaning that surface OH group is also involved in further converting of the CH_3CHO species to HCOO on Ni active sites. The OH groups which spill over to the Ni surface or the Ni/oxides interface can react with CH_3CHO at lower temperatures compared to that without the presence of Ni and OH species because OH groups can reduce the energy barrier for the C–C bond breaking of CH_3COO, forming adsorbed HCOO and CH_4 [56]. Formate can be converted to H_2 and CO_2 finally.

Hence these IR data clearly show that Ni is the active center for the C–C bond scission. Without Ni, C_2 species (CH_3CHO or CH_3COO) remain stable on Ca-Al_2O_3 or Al_2O_3 at relatively high temperatures. Ca addition promotes water adsorption, which can enhance the ethanol adsorption and provide proximity and abundance of surface OH groups

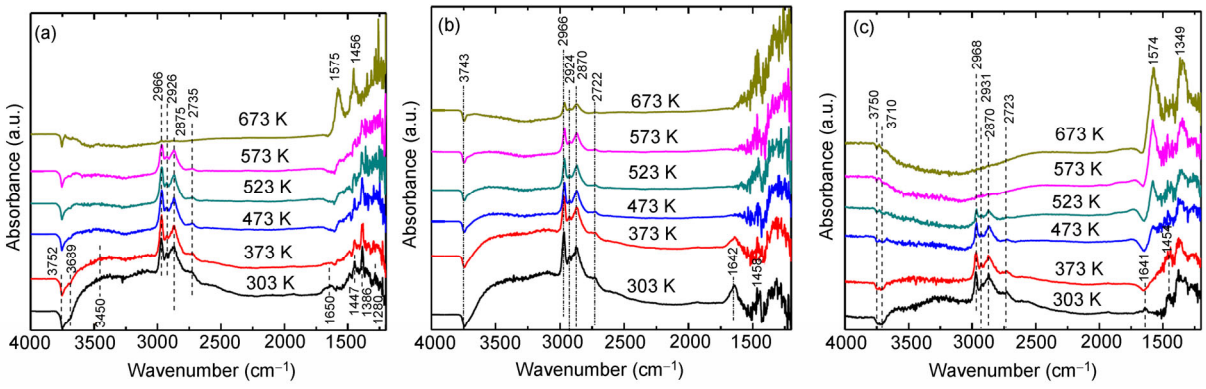

Figure 14 Variable temperature DRIFTS spectra in the region of 4000–1200 cm^{-1} for (a) Al_2O_3, (b) Ca-Al_2O_3 and (c) Ni/Ca-Al_2O_3 after C_2H_5OH adsorption. Each of the spectra was obtained by subtracting the respective DRIFT spectrum prior to the ethanol exposure [15].

to Ni active sites. The surface OH groups can participate and assist in the rapid conversion of adsorbed intermediates CH_3CHO and CH_3CO into CO_2 and CH_4 via adsorbed HCOO and CH_x. Without CaO addition and the presence of abundant OH groups CH_3CHO is converted to acetate and decompose at higher temperatures [18].

5.3 The 10 wt% Ni/3Ca-Al_2O_3 is highly active and stable catalyst for SRE

Increasing Ni loading from 1 wt% to 10 wt% increases the ethanol conversion at 673 K (83.9% on 1 wt% Ni/Al_2O_3 vs. 100% on 10 wt% Ni/Al_2O_3) [16]. High Ni loading (10 wt% Ni) on the other hand causes rapid deactivation of the Ni catalysts (Figure 15) [16]. After 12 h operation over 10 wt% Ni/Al_2O_3 the deactivation occurs. Ethanol conversion declines, the CO_2 and CH_4 selectivities decrease, while that of CH_3CHO and CO increases. These are the disadvantages of supported Ni catalysts.

The addition of 3% CaO greatly improves the catalytic stability and the H_2 production in the wide temperature range. The 10Ni/3Ca-Al_2O_3 remains active during the whole test period, with 100% ethanol conversion and high H_2/CO_2 selectivies (90% of S_{H_2}, 80% of S_{CO_2} and 19% S_{CH_4}) (Figure 15(b)). However, further increase in Ca loading to 5%–7% in 10Ni/5Ca-Al_2O_3 and 10Ni/7Ca-Al_2O_3 leads to a severe loss of the catalytic activity (Figure 15(c, d)).

5.4 The promotion effects of CaO addition and the mechanism of Coke-resistance

CaO addition shows both disadvantages and advantages. On one hand it reduces the surface area of Al_2O_3 (116 m^2/g for bare Al_2O_3 vs. 75.5 m^2/g for 3Ca-Al_2O_3) and weakens the interaction between Ni and Al_2O_3 (as shown by XPS study with lower $NiAl_2O_4$ intensity for the Ni/Ca-Al_2O_3 samples vs. Ni/Al_2O_3). As a result more Ni metal (higher active site density) is located on the top layer surface region and Ni particle becomes bigger on Ca-Al_2O_3 than bare Al_2O_3 (5.8 nm for 10Ni/3Ca-Al_2O_3 and 6.4 nm for 10Ni/7Ca-Al_2O_3 vs. 2.4 nm for 10Ni/Al_2O_3). On the other hand, electronic enrichment in Ni 3d electrons (in the binding energy region 0–5 eV) is found in UPS spectra on Ca-modified catalysts and increased with Ca loading (Figure 16), which is in favour of the activation of C–C and C–H bonds.

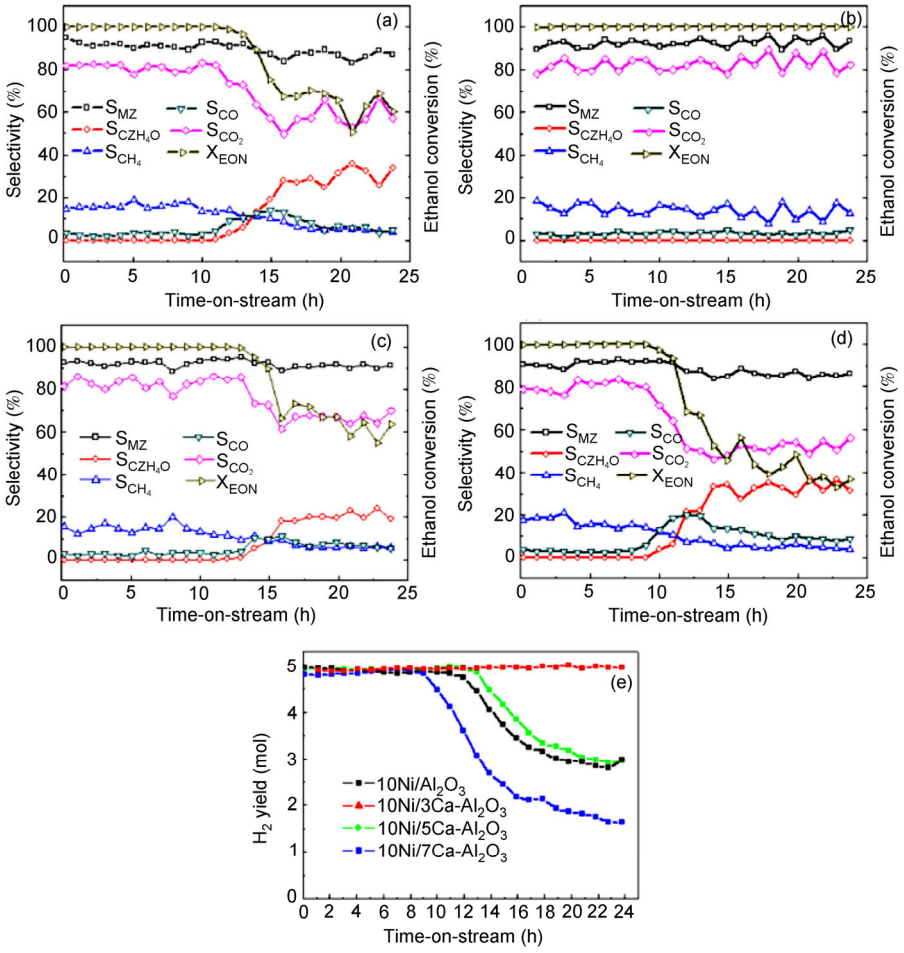

Figure 15 Catalytic performance of (a) 10Ni/Al_2O_3, (b) 10Ni/3Ca-Al_2O_3, (c) 10Ni/5Ca-Al_2O_3, (d) 10Ni/7Ca-Al_2O_3 as well as in (e) H_2 yield of the above catalysts. Reaction at 673 K with ethanol/water ratio at 1:3 by volume [16].

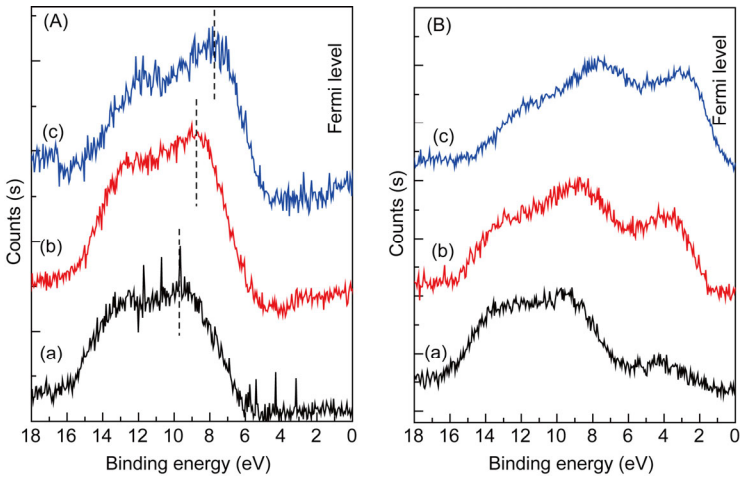

Figure 16 Valence band of (A) Ni-free and (B) Ni catalysts supported on (a) Al_2O_3, (b) 3Ca-Al_2O_3 and (c) 7Ca-Al_2O_3 [16].

Thus the Ca addition can promote not only the conversion of acetaldehyde (to CO and CH_4) but also methane decomposition (to carbon deposition). At 673 K the S_{CH_3CHO} decreases from 37.9% for Ni/Al_2O_3 to 0.91% for Ni/Ca-Al_2O_3 while S_{CH_4} increases from 18.5% for Ni/Al_2O_3 to 33.5% for Ni/Ca-Al_2O_3 (Table 4). Methane becomes the main product of SRE at low temperatures (673 K) in addition to H_2 (73.2%) and CO_2 (59.4%). Methane is also the main source of coke precursors in this case since the selectivity of other coke precursors is rather low (0.91% of CH_3CHO, zero of C_2H_4 and 6.2% of CO). The CH_4-derived coking rate (measured by a TGA study in Figure 17) is found to increase with increasing Ni particle size, following the sequence of 10Ni/7Ca-Al_2O_3>10Ni/3Ca- Al_2O_3>10Ni/Al_2O_3. Luckily, the presence of CaO can promote the steam gasification via water-gas-shift during SRE. As shown in Figure 17 [16], the gasification of coke on Ni/Al_2O_3 begins at 675 K, while the set-on temperature dramatically reduces (by 80°) to 595 K for Ca-promoted catalysts. This means that the coke on Ca-promoted catalyst is easier to be removed, leaving more active Ni particles exposed for reaction on 10Ni/3Ca-Al_2O_3 catalyst. Therefore, the excellent stability of 10Ni/3Ca-Al_2O_3 is due to the optimization of Ca-loading such that coke deposition via CH_4 decomposition is minimized while maintaining a steady gasification of coke deposits by steam.

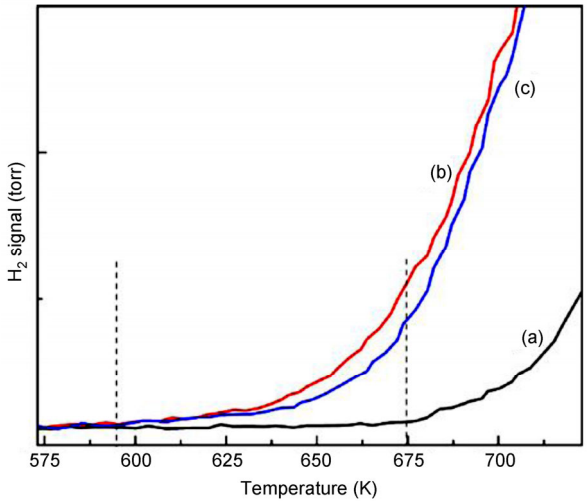

Figure 17 Steam gasification of coke produced from CH_4 decomposition on (a) 10Ni/Al_2O_3, (b) 10Ni/3Ca-Al_2O_3 and (c) 10Ni/7Ca-Al_2O_3 [16].

6 The reaction pathways for SRE on Ni, Pt, Rh and Pd supported on Ca-Al_2O_3

The reactivity of ethanol and the process intermediates in each elementary step of SRE depends very much on the structural and electronic properties of the catalyst. Therefore on various catalysts the preferred reaction pathways and hence the products distribution are often different. Nevertheless there exist similarities and several common reaction teps on various types of the catalysts.

One generally proposed mechanism involves the participation of acetates via dehydrogenation and subsequent oxidation from ethoxides. On modelled catalytic surfaces of Ni, Pt and other noble metals, ethanol decomposition was shown to proceed in the following order of bond breaking: O–H, αC–H, C–C and βC–H [43–45]. Hence the preferred αC–H bond breaking may result in the formation of acetaldehyde and acetyl intermediates from ethoxide. Ethoxide can either decompose into H_2, CO, and CH_4 or undergo dehydrogenation, producing acetaldehyde and acetyl, which may further react with lattice oxygen or surface hydroxyls, leading to formation of the acetate intermediate and the final products CO_2 and CH_4. The existence of the acetate species is often demonstrated in IR spectra with characteristic vibrations at 1575 and 1460 cm^{-1} [18] (Figure 18(a)). This reaction pathway is generally accepted as the acetate inter-

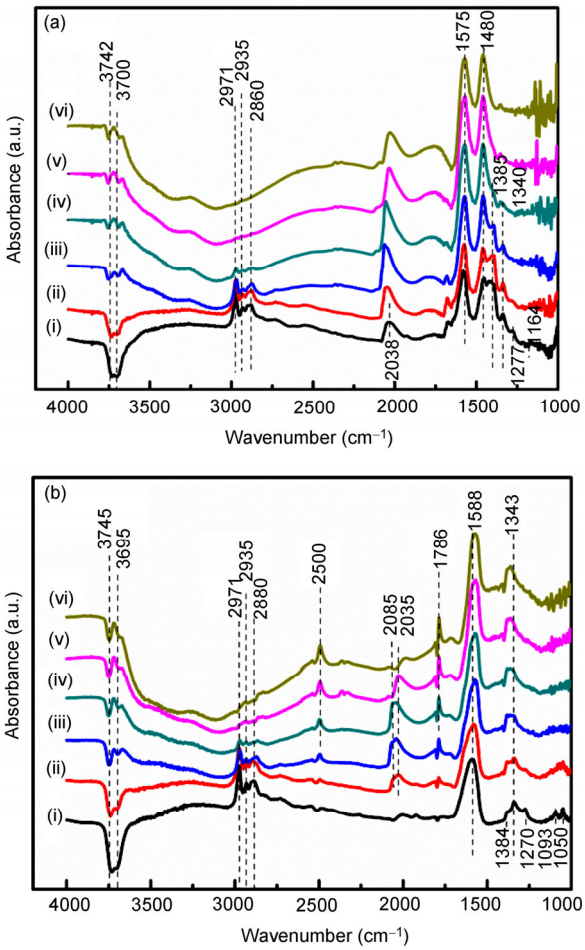

Figure 18 DRIFT spectra at various temperatures after C_2H_5OH adsorption on (a) Pt/Al_2O_3, and (b) $Pt/Ca\text{-}Al_2O_3$. The spectra were recorded at (i) 303 K after ethanol adsorption followed by He purge and (ii–vi) 373, 473, 523, and 675 K, respectively [18].

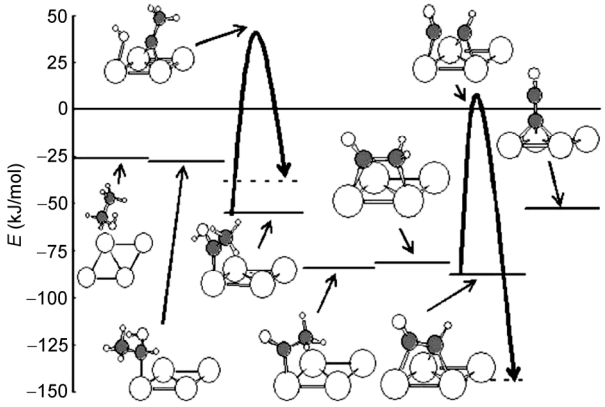

Figure 19 Reaction energy diagram for ethanol reactions on Pt(111). The reference state is gas phase ethanol and clean slab(s). Removed H atoms and bond cleavage products are each adsorbed on separate slabs. Solid curves represent bond cleavage reactions. Insets show views of stable and transition state species. The large white circles represent Pt atoms, grey medium circles represent C atoms, white medium circles represent O atoms, and the small white circles represent H atoms [8].

mediate pathway. Figure 19 provides an energy potential diagram for ethanol surface reaction on Pt(111), which follows the acetate intermediate pathway.

Recently, the existence of formate species as the SRE intermediate alternative to the acetate intermediate (as observed on Pt/Al_2O_3) was noted on Al_2O_3-supported Pt catalysts [57,58], unreduced Pt/CeO_2 [59], Fe-promoted $Rh/CaAl_2O_3$ [10,15] and $Pt/Ca\text{-}Al_20_3$ catalyst [18]. Chen *et al.* [18] therefore proposed a new pathway for SRE and denoted it as the formate-intermediate mechanism. The existence of the formate species is easily detected via *in-situ* DRIFT studies. Figure 18(b) displays the IR spectra of ethanol adsorption on $Pt/Ca\text{-}Al_2O_3$ at various temperatures. The appearance of adsorbed ethanol, ethoxides, and the negative OH bands is similar to that on Pt/Al_2O_3 in Figure 18(a). However, there are two significant differences for $Pt/Ca\text{-}Al_2O_3$. First, the characteristic acetate band at 1460 cm^{-1} is not observed. Instead, two predominant bands at 1575–1588 and 1340–1360 cm^{-1} are clearly ascribed to the asymmetric and symmetric O–C–O stretching vibrations, respectively, of formate species. Secondly the CO band at 2036 cm^{-1} which is strong in Figure 18(a) is not evident on $Pt/Ca\text{-}Al_2O_3$ at 303 K in Figure 18(b). CO adsorption is associated with the dissociation of ethoxide species. The smaller amount of adsorbed CO on $Pt/Ca\text{-}Al_2O_3$ at 303 K suggests that ethoxide species are more stable on $Pt/Ca\text{-}Al_2O_3$ than on Pt/Al_2O_3 due to the higher affinity for water adsorption on the Ca-modified catalysts. Progressive heating of the sample leads to the increase in CO adsorption on $Pt/Ca\text{-}Al_2O_3$ between 373 and 523 K, being parallel to the loss of adsorbed ethanol and ethoxide species. The CO bands starts to decline at ⩾573 K. At 473 K, two new bands at 2500 and 1786 cm^{-1} are observed. They are assigned to the H–OC and HC=O stretches of adsorbed HCO species, respectively. The formation of HCO will require the cleavage of the C–C bond with the assistance of active metal sites. The presence of abundant surface OH groups can aid the conversion of adsorbed CO or HCO species to formate species HCOO, which may then undergo either dehydration (to CO) or dehydrogenation (to H_2 and CO_2), depending on the structure of the formate [19]. The formate species on $Pt/Ca\text{-}Al_2O_3$ are bidentate, which can be converted to CO_2 and H_2 upon heating. These spectroscopic evidences clearly show that the Ca modification of alumina has altered the reaction pathway of SRE from the acetate intermediate route over Pt/Al_2O_3 to the formate-intermediate over $Pt/Ca\text{-}Al_2O_3$.

The formate-intermediate pathway is also observed over $Ca\text{-}Al_2O_3$ supported Ni, Rh and Pd catalysts [15,18]. This may suggest that formate formation is independent of the nature of the active metals, which is consistent with the conclusion that the formation of surface acetates over Al_2O_3-supported Rh, Ir, Ru, Pd, and Pt catalysts is independent of the nature of the active metals [60]. Therefore, the change from the acetate- to formate- intermediated pathway is solely related to the changes in the surface prop-

erties of the support induced by Ca addition.

The formation of acetates from ethanol adsorption has been widely reported over various oxides, such as Al_2O_3, MgO, and CeO_2 [61, 62]. The high availability of oxygen atoms on the support is the key which favours the oxidation of carboxyl carbon to acetate. Yee *et al*. [63] studied ethanol adsorption over unreduced CeO_2, reduced CeO_2, and Pd/CeO_2. Their results show that surface oxygen atoms on unreduced CeO_2 are responsible for acetate formation. On the other hand, the formation of acetate is not observed on the reduced CeO_2 and Pd/CeO_2 because of the depletion of surface oxygen atoms.

Similarly, on the surface of the Pt/Al_2O_3 with no CaO modification there are large numbers of surface oxide ions in close interaction with the adsorbed ethoxide/acetaldehyde, favouring the formation of acetate species. The presence of Ca induces significant changes in the surface properties, thereby altering the reaction pathway. Ca modification on Al_2O_3 increases Ni concentrations on the surface and 3d electron density near the Fermi level, promoting the C–C bond cleavage of adsorbed C2 intermediates. It facilitates the water adsorption and availability of abundant surface OH groups which helps the formation and conversion (to H_2 and CO_2) of adsorbed formate. Hence, ethanol reaction on $Ca\text{-}Al_2O_3$-supported Ni, Pt, Pd and Rh catalysts follows the new formate-intermidated reaction pathway shown in Scheme 1 [18].

7 Conclusions

In this paper the application of molecular catalysis for SRE is summarized. H_2 derived from bio-ethanol via SRE is a sustainable clean energy for future transportation and power plants. SRE is kinetic controlled and needs a good catalyst to achieve high ethanol conversion, high H_2 selectivity, low cost and long catalyst life span. The catalysts for SRE roughly include four groups, namely metal oxides, metal-oxide-supported base metals, noble metals and alloys. ZnO alone is one of the best metal-oxide catalysts for SRE. However, the presence of metal such as Co is found to further improve its SRE performance. In the supported metal catalysts, only 8 metals (Ni, Co, Cu, Pt, Rh, Pd, Ir and Ru) have shown high catalytic activity for the H_2 production via SRE. Among them, Ni and Rh are the two very promising metal catalysts because they can effectively promote C–C bond cleavage during SRE, due to high d character in the metal bond and low metal-oxygen bonding (vs. metal-carbon). However, Rh is weak in water-gas-shift so that CH_4 and CO become the main by-products of SRE at low reaction temperatures. We have developed two low-temperature CO-free catalysts in our lab, namely $Rh\text{-}Fe/Ca\text{-}Al_2O_3$ and carbonyl-derived $Rh\text{-}Co/CeO_2$, in which iron-oxide promoter or Co as the 2nd metal in the catalysts can assist Rh metal to promote water-gas-shift reaction and significantly improve the SRE performance.

Ni is strong in activate C–C and C–H bonds. Ni/Al_2O_3 is an economic and excellent catalyst for SRE. However, rapid deactivation of the Ni catalysts inhibits its practical applications. The addition of 3 wt% CaO to Al_2O_3 is found to solve the problems because the Ca modification increases Ni concentrations on the surface and 3d electron density near the Fermi level, promoting the C–C bond cleavage of adsorbed C2 intermediates. It also facilitates the water adsorption and availability of abundant surface OH groups which help the formation and conversion (to H_2 and CO_2) of adsorbed formate as well as the coke gasification. Hence, ethanol reaction on $Ca\text{-}Al_2O_3$-supported Ni, Pt, Pd and Rh catalysts follows formate-intermediated pathway, a new reaction pathway alternative to the traditional acetate-intermediated pathway such as that on Al_2O_3-supported Pt.

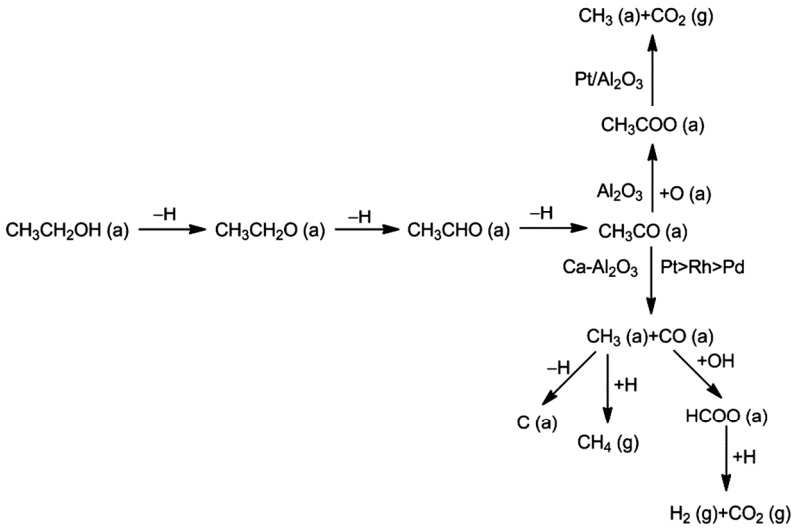

Scheme 1 Reaction pathways of ethanol over Al_2O_3- and $Ca\text{-}Al_2O_3$-supported noble metals.

Lin Jianyi sincerely thanks for the continuous encourage and guidance during his entire academic career from his mentor Academician Prof. Tsai Qi Rui of Xiamen University. The funding from the Institute of Chemical and Engineering Sciences, Singapore, to support the project "Alcohol Reforming for Hydrogen Generation" is also acknowledged.

1 Note: If 1 liter of pure ethanol (density 0.79 g/mL) is used directly as a fuel of heat engines, only about 20% of the chemical energy stored in ethanol can be converted to useful mechanical work. This will generate 4392 kJ of energy (per liter) by assuming the enthalpy of combustion is 1277 kJ/mol for ethanol. On the other hand, 1 liter of ethanol can be converted to 92.85 mole of H_2 (assuming 90% H_2 selectivity in SRE) and will produce 12829 kJ energy (assuming 60% the fuel cell efficiency).
2 Sun J, Wang Y. Recent advances in catalytic conversion of ethanol to chemicals. *ACS Catal*, 2014, 4: 1078–1090
3 Kumar A, Prasad R, Sharma YC. Steam reforming of ethanol: production of renewable hydrogen. *Int J Environ Res Dev*, 2014, 4: 203–212
4 Mattos LV, Jacobs G, Davis BH, Noronha FB. Production of hydrogen from ethanol: review of reaction mechanism and catalyst deactivation. *Chem Rev*, 2012, 112: 4094–4123
5 Trane R, Dahl S, Skjoth-Rasmussen MS, Jensen AD. Catalytic steam reforming of bio-oil. *Int J Hydrogen Energy*, 2012, 37: 6447–6472
6 Ni M, Leung DYC, Leung MKH. A review on reforming bio-ethanol for hydrogen production *Int J Hydrogen Energy*, 2007, 32: 3238–3247
7 Vaidya PD, Rodrigues AE. Insight into steam reforming of ethanol to produce hydrogen for fuel cells. *Chem Eng J*, 2006, 117: 38–49
8 Davda PR, Shabaker JW, Huber GW, Cortrighti RD, Dumesic JA. A review of catalytic issues and process conditions for renewable hydrogen and alkanes by aqueous-phase reforming of oxygenated hydrocarbons over supported metal catalysts *Appl Catal B*, 2005, 56: 171–176
9 Haryanto A, Fernando S, Murali N, Adhikari S. Current status of hydrogen production techniques by steam reforming of ethanol: a review. *Energy Fuels*, 2005, 19: 2098–2106
10 Koh ACW, Leong WK, Chen L, Ang TP, Lin J, Johnson BFG, Khimyak T. Highly efficient ruthenium and ruthenium-platinum cluster-derived nanocatalysts for hydrogen production via ethanol steam reforming. *Catal Commun*, 2008, 9: 170–175
11 Zhong ZY, Ang H, Choong CKS, Chen L, Huang L, Lin J. The role of acidic sites and the catalytic reaction pathways on the Rh/ZrO_2 catalysts for ethanol steam reforming. *Phys Chem Chem Phys*, 2009, 11: 872–880
12 Huang L, Choong CKS, Chen L, Wang Z, Zhong Z, Cuerva CC, Lin J. Monometallic carbonyl-derived CeO_2-supported Rh and Co bicomponent catalysts for CO-free, high-yield H_2 generation from low-temperature ethanol steam reforming. *ChemCatChem*, 2013, 5: 220–234
13 Chen L, Choong CKS, Zhong Z, Huang L, Ang TP, Hong L, Lin J. Carbon monoxide-free hydrogen production via low-temperature steam reforming of ethanol over iron-promoted Rh catalyst. *J Catal*, 2010, 276: 197–200
14 Choong CKS, Chen L, Du Y, Wang Z, Hong L, Borgna A. Rh-Fe/Ca-Al_2O_3: a unique catalyst for CO-free hydrogen production in low temperature ethanol steam reforming. *Top Catal*, 2014, 57: 627–636
15 Choong CKS, Huang L, Zhong Z, Lin J, Hong L, Chen L. Effect of calcium addition on catalytic ethanol steam reforming of Ni/Al_2O_3: II. Acidity/basicity, water adsorption and catalytic activity. *Appl Catal A: General*, 2011, 407: 155–162
16 Choong CKS, Zhong Z, Huang L, Wang Z, Ang TP, Borgna A, Lin J, Hong L, Chen L. Effect of calcium addition on catalytic ethanol steam reforming of Ni/Al_2O_3: I. Catalytic stability, electronic properties and coking mechanism. *Appl Catal A: General*, 2011, 407: 145–154
17 Chen L, Choong CKS, Zhong Z, Huang L, Wang Z, Lin J. Support and alloy effects on activity and product selectivity for ethanol steam reforming over supported nickel cobalt catalysts. *Int J Hydrogen Energy*, 2012, 37: 16321–16332
18 Choong CKS, Zhong Z, Huang L, Borgna A, Hong L, Chen L, Lin J. Infrared evidence of a formate-intermediate mechanism over Ca-modified supports in low-temperature ethanol steam reforming. *ACS Catal*, 2014, 4: 2359–2363
19 Lin J, Neoh KG, Teo WKJ. Thermogravimetry-FTIR study of the surface formate decomposition on Cu, CuCl, Cu_2O and CuO correlations between reaction selectivity and structural properties. *Chem Soc, Faraday Trans*, 1994, 9: 355–362
20 Fishtik I, Alexander A, Datta R, Geana D. A thermodynamic analysis of hydrogen production by steam reforming of ethanol via response reactions. *Int J Hydrogen Energy*, 2000, 25: 31–45
21 Garcia EY, Laborde MA. Hydrogen production by the steam reforming of ethanol: thermodynamic analysis. *Int J Hydrogen Energy*, 1991, 16: 16–307
22 Vasudeva K, Mitra N, Umansankar P, Dhingra SC. Steam reforming of ethanol for hydrogen production: thermodynamic analysis. *Int J Hydrogen Energy*, 1996, 21: 13–18
23 Vaidya PD, Rodrigues AE. Insight into steam reforming of ethanol to produce hydrogen for fuel cells. *Chem Eng*, 2006, 17: 39–49
24 Singhto W, Laosiripojana N, Assabumrungrat S, Charojrochkul S. Steam reforming of bio-ethanol over Ni on Ce-ZrO_2 support: influence of redox properties on the catalyst reactivity. *Songklanakarin J Sci Technol*, 2006, 28: 1251–1264
25 Llorca J, Piscina PR de la, Sales J. Homs direct production of hydrogen from ethanolic aqueous solutions over oxidecatalysts N. *Chem Commun*, 2001: 641–642
26 Llorca J, Piscina PR de la, Dalmon JA, Sales J, Homs N. CO-free hydrogen from steam-reforming of bioethanol over ZnO-supported cobalt catalysts effect of the metallic precursor. *Appl Catal B*, 2003, 43: 355–369
27 Llorca J, Homs N, Piscina PR de la. *In situ* DRIFT-mass spectrometry study of the ethanol steam-reforming reaction over carbonyl-derived Co/ZnO catalysts. *J Catal*, 2004, 27: 556–560
28 Vecchietti J, Bonivardi A, Xu W, Stacchiola D, Delgado JJ, Calatayud M, Collins SnE. Understanding the role of oxygen vacancies in the water gas shift reaction on ceria-supported platinum catalysts. *ACS Catal*, 2014, 4: 2088–2096
29 Llorca L, Homs N, Sales J, Piscin PR de la. Efficient production of hydrogen over supported cobalt catalysts from ethanol steam reforming. *J Catal*, 2002, 209: 306–317
30 Wang Z, Wang H, Liu Y. $La_{1-x}Ca_xFe_{1-x}Co_xO_3$: a stable catalyst for oxidative steam reforming of ethanol to produce hydrogen. *RSC Adv*, 2013, 3: 10027–10036
31 Xu W, Liu Z, Johnston-Peck AC, Senanayake SD, Zhou G, Stacchiola D, Stach EA, Rodriguez JA. Steam reforming of ethanol on Ni/CeO_2: reaction pathway and interaction between Ni and the CeO_2 support. *ACS Catal*, 2013, 3: 975–984
32 Cavallaro S. Ethanol steam reforming on Rh/Al_2O_3 catalysts. *Energ Fuel*, 2000, 14: 1195–1199
33 Duan S, Senkan S. Catalytic conversion of ethanol to hydrogen using combinatorial methods. *Ind Eng Chem Res*, 2005, 44: 6381–6386
34 Auprêtre F, Descorme C, Duprez D. Bio-ethanol catalytic steam reforming over supported metal catalysts. *Catal Comm*, 2002, 3: 263–267
35 Liguras DK, Kondarides DI, Verykios XE. Production of hydrogen for fuel cells by steam reforming of ethanol over supported noble metal catalysts. *Appl Catal B*, 2003, 43: 345–354
36 Basagiannis AC, Panagiotopoulou P, Verykios XE. Low temperature steam reforming of ethanol over supported noble metal catalysts. *Top Catal*, 2008, 51: 2–12
37 Frusteri F, Freni S, Spadaro L, Chiodo V, Bonura G, Donato S, Cavallaro S. H_2 production for MC fuel cell by steam reforming of ethanol over MgO supported Pd, Rh, Ni and Co catalysts. *Catal Commun*, 2004, 5: 611–615

38 Idriss H. Ethanol reactions over the surfaces of noble metal/cerium oxide catalysts. *Platin Met Rev*, 2004, 48: 105–115
39 Ferrin P, Simonetti D, Kandoi S, Kunkes E, Dumesic JA, Nørskov JK, Mavrikakis M. Modeling ethanol decomposition on transition metals: a combined application of scaling and Brønsted-Evans-Polanyi relations. *J Am Chem Soc*, 2009, 131: 5809–5815
40 Mavrikakis M, Barteau MA. Oxygenate reaction pathways on transition metal surfaces. *J Mol Catal A: Chem*, 1998, 131: 135–147
41 Sinfelt JH, Yates JC. Catalytic hydrogenolysis of ethane over noble metals of Group VIII. *J Catal*, 1967, 8: 85–90
42 Sinfelt JH, Taylor WF, Yates DJC. Catalysis over supported metals. III. Comparison of metals of known surface area for ethane hydrogenolysis. *J Phys Chem*, 1965, 69: 95–101
43 Gates SM, Russell JN, Yates Jr JT. Bond activation sequence observed in the chemisorption and surface reaction of ethanol on Ni(111). *Surf Sci*, 1986, 171: 111–134
44 Maŕrikakis M, Barteaur MA. Oxygenate reaction pathways on transition metal surfaces. *J Mol Catal A: Chem*, 1998, 131: 135–147
45 Davis L, Barteau MA. The influence of oxygen on the selectivity of alcohol conversion on Pd(111) surface. *Sur Sci*, 1988, 197: 123–152
46 Alcalá R, Mavrikakis M, Dumesic JA. DFT studies for cleavage of C–C and C–O bonds in surface species derived from ethanol on Pt(111). *J Catal*, 2003, 218: 178–190
47 Morton D, Cole-Hamilton DJ, Utuk ID, Paneque-Sosa M, Manuel L. Hydrogen production from ethanol catalysed by Group 8 metal complexes. *J Chem Soc*, *Dalton Trans*, 1989, 3: 489–495
48 Deluga GA, Salge JR, Schmidt LD, Verykios XE. Renewable hydrogen from ethanol by autothermal reforming. *Science*, 2004, 303: 993–997
49 Ferencz Zs, Erdohelyi A, Baan K, Oszko A, Ovari L, Konya Z, Papp C, Steinruck HP, Kiss J. Effects of support and Rh additive on Co-based catalysts in the ethanol steam reforming reaction. *ACS Catal*, 2014, 4: 1205−1218
50 Senanayake SD, Evans J, Agnoli S, Barrio L, Chen TL, Hrbek J, Rodriguez JA. Water-gas shift and CO methanation reactions over Ni-CeO_2(111) catalysts. *Top Catal*, 2011, 54: 34–41
Han X, Yu Y, He H, Shan W. Hydrogen production from oxidative steam reforming of ethanol over rhodium catalysts supported on Ce-La solid solution. *Int J Hydrogen Energy*, 2013, 38: 10293–10304
51 Aupretre F, Descorme C, Duprez D, Casanave D, Uzio D. Ethanol steam reforming over $Mg_xNi_{1-x}Al_2O_3$ spinel oxide-supported Rh catalysts. *J Catal*, 2005, 233: 464–477
52 Duprez D. Selective steam reforming of aromatic compounds on metal catalysts. *Appl Catal A: Gen*, 1992, 82: 111–157
53 Martin D, Duprez D. Mobility of surface species on oxides. 1. Isotopic exchange of $^{18}O_2$ with ^{16}O of SiO_2, Al_2O_3, ZrO_2, MgO, CeO_2, and CeO_2-Al_2O_3. Activation by noble metals. Correlation with oxide basicity. *J Phys Chem*, 1996, 100: 9429–9438
54 Rostrup-Nielsen JR. Activity of nickel catalysts for steam reforming of hydrocarbons. *J Catal*, 1973, 31: 173–199
55 Sutton JE, Panagiotopoulou P, Verykios XE, Vlachos DG. Combined DFT. Micro-kinetic, and experimental study of ethanol steam reforming on Pt. *J Phys Chem C*, 2013, 117: 4691–4706
56 Panagiotopoulou P, Verykios XE. Mechanistic aspects of the low temperature steam reforming of ethanol over supported Pt catalysts. *Int J Hydrogen Energ*, 2012, 37: 16333–16345
57 Sanchez-Sanchez MC, Yerga RMN, Kondarides DI, Verykios XE, Fierro JLG. Mechanistic aspects of the ethanol steam reforming reaction for hydrogen production on Pt, Ni, and Pt-Ni catalysts supported on γ-Al_2O_3. *J Phys Chem A*, 2010, 114: 3873−3882
58 Yee A, Morrison SJ, Idriss H. A study of ethanol reaction over Pt/CeO_2 by temperature-programmed desorption and *in situ* FT-IR spectroscopy: evidence of benzene formation. *J Catal*, 2000, 191: 30–45
59 Erdo helyi A, Raskó J, Kecskés T, Tóth M, Domok M, Baán K. Hydrogen formation in ethanol reforming on supported noble metal catalysts. *Catal Today*, 2006, 116: 367−376
60 Kagel RO. Infrared investigation of the adsorption and surface reactions of the C1 through C4 normal alcohols on γ-alumina. *J Phys Chem*, 1967, 71: 844–850
61 Kagel RO, Greenler RG. Infrared study of the adsorption of methanol and ethanol on magnesium oxide. *J Chem Phys*, 1968, 49: 1638–1647
62 Yee A, Morrison SJ, Idriss H. A study of the reaction of ethanol on CeO_2 and Pd/CeO_2 by steady state react ions, TPD and *in-situ* FT-IR. *J Catal*, 1999, 186: 279–295